Investigation of the Role of $Gd_2Zr_2O_7$ (GZ) Powders in Thermal Cycling Behavior of Thermal Barrier Coatings

By

Swamy Nandikolla

A thesis

Presented to

The Faculty of Engineering

In Partial Fulfillment of

The Requirements for the Degree

Master of Engineering

Southern University and A&M College

Department of Mechanical Engineering

Baton Rouge, LA, USA

July. 2012

The Graduate School
Southern University and A&M College
Baton Rouge, Louisiana

CERTIFICATE OF APPROVAL

MASTER'S THESIS

This is to certify that the Master's Thesis of

Swamy Nandikolla

has been approved by the Examining Committee for the thesis

requirement for the Master of Engineering degree in

Mechanical Engineering, July 2012

Name: **Dr. Patrick F. Mensah** Date
CHAIR, Thesis Committee

Name: **Dr. Ravinder M. Diwan** Date
Committee Member

Name: **Dr. Samuel Ibekwe** Date
Committee Member

Name: **Dr. Samuel Ibekwe** Date
Department Chair

Name: **Dr. Habib. P. Mohamadin** Date
Dean, College of Engineering

Name: **Dr. Mwalimu J. Shujaa** Date
Dean of the Graduate School

This Research was supported by

Department of Energy (DoE) - Grant number DE-FC26-08NTO1922) 2007-Present

and

NASA Experimental Program to Stimulate Competitive Research (EPSCoR)- Grant number NNX09AP72A

Investigation of the Role of $Gd_2Zr_2O_7$ (GZ) Powders in Thermal Cycling Behavior of Thermal Barrier Coatings

By

Swamy Nandikolla

A thesis

Presented to

The Faculty of Engineering

In Partial Fulfillment of

The Requirements for the Degree

Master of Engineering

Southern University and A&M College

Department of Mechanical Engineering

Baton Rouge, LA, USA

July. 2012

ABSTRACT

Thermal barrier coatings (TBCs) are used in gas turbine engines to extend the performance limits of current super alloys thereby increasing engine efficiency and performance. In this thesis the thermal cycling life and mechanical properties of functionally graded Gadolinium-Zirconate (GZ) + Yattria-stabilized-zirconia (YSZ) double layer TBCs in addition to pure YSZ and pure GZ TBCs are investigated and analyzed. Functionally graded TBC samples are made of 10, 25, 50, 75 wt% GZ/YSZ powder ratio. All the samples used in this work are fabricated using standard air plasma spraying (APS) technique. The porosity of these TBCs is characterized quantitatively by mercury intrusion porosimetry using Poremaster 33 analyzer. Mechanical properties such as elastic modulus and hardness are measured by nano indentation on the cross-section of the coating specimens. Thermal cycling behavior of these TBCs was tested at 1100^{o}C with and without temperature gradient. The temperature gradient thermal cycling tests are carried out in a novel thermal cycling furnace for controlled temperature gradient and environment. The isothermal cycling tests are carried out in CM 1700 bottom loading furnace. A Scanning Electron Microscope (SEM) was used to study the microstructure of the failed samples. The hardness test results indicate a trend of possible benefits of GZ addition up to 50% in the measured double layer TBCs. The results of the temperature gradient thermal cycling indicate that at high surface temperatures (1100^{o}C) the functionally graded GZ based double layer TBC system meets the expectations, as the thermal cycling performance is similar to those of YSZ TBCs indicating that addition of

GZ in double layer TBC system improves the life of GZ based TBCs besides lower thermal conductivity and providing beneficial insulating TBC properties for high temperature applications.

ACKNOWLEDGEMENTS

No creation in this world is a solo effort. Neither is this work. It would not have been possible to write this master's thesis without the help and support of the people around me.

I would like to express my sincere gratitude to my principal advisor, Prof. Patrick F Mensah, not to mention his support, patience and enthusiasm. I would also like to express my gratitude to my committee co-chair Dr. Ravinder M. Diwan for his good advice, immense knowledge and his great efforts to explain things clearly and simply. His support has been invaluable on both academic and a personal level, for which I am extremely grateful. I would also like to thank my thesis committee member and chair of Mechanical Engineering, Southern University, Dr. Samuel Ibekwe for his advocacy throughout my academic program and research. I am also extremely indebted to Dr. S. M. Guo, Louisiana State University for providing necessary infrastructure and resources to accomplish part of my research work.

I would like to thank Dr. Stephen Akwaboa for his encouragement and insightful comments throughout my thesis work. Temperature gradient thermal cycling testing in this thesis would not have been possible without a close collaboration with Engineering Research and development laboratory at Louisiana State University, supported by Dr. Guo. My thanks are due to Mr. Williams Liang and Mr. Hamed Habibi for sharing laboratory equipment at Louisiana State University. I take this opportunity to sincerely

acknowledge Mr. Fareed Dawan, Mr. Niteesh Morampudi and Mr. Ali Ghamsari for their support during my experimentation at NextgenC^3 laboratory, Southern University.

Thanks are expresses to my family for their belief and support of my work .I would like to express my deep gratitude to late Dr. Vishawa Mohan, you have been a tremendous mentor for me. Your advice on both research as well as on my career have been invaluable. I would also like to thank my friends from college, team members and my roommates, especially Dr. Ram Kishore, Mr.Aravind Vemisetty and Mr. Sarat Paluri for their help with the editing of this document. Words are short to express my deep sense of gratitude towards my following friends Naresh Polasa, Sangeetha Gudla and Vamsi Achanta.

Last, but by no means least, I would like to thank my mentor, inspiration and friend Wang Li for the simulating discussions on research, for the late hours we worked together in the research laboratory, and for all the fun we had for the last two years.

CONTENTS

LIST OF TABLES

LIST OF FIGURES

CHAPTER I

INTRODUCTION

1.1 Background

The worldwide demand for power is growing faster than the world's population. Since the early nineties a strong trend towards gas turbine application for power generation could be noticed. The more complex the advanced gas turbines got, the higher the turbine inlet temperature was pushed. The more exotic cooling technique and materials had to be applied. To reach the high process temperature of advanced gas turbines , necessary to achieve postulate engine efficiencies, could only be realized by applying combined measures to the most exposed parts as first row turbine vanes and blades to withstand the heat. The measures include the choice of heat –resistant alloys, efficient cooling of the vane and blade metal structure, and a thermal insulation layer- referred as Thermal barrier coating (TBC) to protect the metal components from the direct heat impact of the combustion gases.

Thermal Barrier Coatings are widely used as a protective coating for turbine parts. Development of these thermal barrier coatings started in 1950s and has been an attractive research area for many decades for the researchers. Typical thermal barrier coatings consist of two layers. The bottom layer is called Bond Coat which acts as a bonding between the metallic substrate and the top coat and also protects the metallic substrate from corrosion and oxidation. The top layer is a ceramic topcoat which acts a thermal

barrier for protecting the turbine components. Currently two processes are widely used to fabricate the top coat of these systems: atmospheric plasma spraying (APS) and Electron beam physical vapor deposition (EB-PVD). During the fabrication process of the bond coat on the substrate a thermally grown oxide TGO is formed which introduces additional stress levels in the TBC system. Research has been advancing in studying the adverse changes that occur due to thermo mechanical treatment of these different components-substrate, bond coat and top coat in hazardous environment of a gas turbine[2].

Six to eight % YSZ is a traditional TBC top coat candidate for gas turbine applications from 1970s. Though YSZ has been very successful for TBC applications some of the disadvantages include an adverse effect of sintering on the performance of YSZ. Due to sintering effects the strain tolerance reduces along with an increase in the Young's modulus which leads to higher stresses in the coatings which leads to reduce the thermal cycling life [2].

Research is ascending in search of new class of advanced TBC materials to overcome the disadvantages of YSZ. Rare-earth zirconates with a general formula $R_2Zr_2O_7$ (R=rare earth), crystalline in the ordered pyrochlore structure with lower thermal conductivity and higher phase stability than those of the conventional YSZ ceramics are identified as promising candidates as alternate TBC ceramics.

$Gd_2Zr_2O_7$ Gadolinium Zirconate (GZ) shows promising thermo physical properties, i.e., lower thermal conductivity than YSZ and high thermal stability. In spite

of these advantages the coefficient of thermal expansion (CTE) of GZ (9-10 x 10^{-6}/k) is lower than that of YSZ (10-11 x 10^{-6}/k) that results in high thermal stresses in the TBC system as both the substrate and the bond coat have a higher CTE value (about 15 x 10^{-6}/k).In addition, relatively lower toughness values are observed in GZ. As a result, the thermal cycling properties are worse than those of YSZ coatings. One possible approach to resolve this problem is to use layered coatings within the TBC system. Failure of TBC systems often occur within the TBC close to the bond coat/top coat interface. YSZ layer is coated to overcome the lower CTE and toughness issues with GZ. The YSZ layer is then coated with GZ layer which has high thermal stability. However to improve the double layered concept to a new level, functional gradient TBCs with a gradual compositional variation are proposed to mitigate these problems even better. The YSZ layer is coated with functionally graded GZ+YSZ coating. There is a need to find the appropriate function for this composition of YSZ+GZ to overcome the issue of lower CTE of single layer GZ.

1.2 Objective

Thermal barrier coatings have been the subject of vigorous research over the past few years. The main intention is to enhance the reliability of TBCs so that they can be effectively used at higher operating temperatures anticipated for the next generation gas turbines. The menu of the candidate materials and architecture has expanded considerably, including the materials from the zirconia family with increased temperature capability, functionally graded coating techniques.

As a main objective of this thesis, the thermal cycling life and mechanical properties of functionally graded GZ+ YSZ TBC coatings in addition to single layer GZ and YSZ TBCs are investigated and analyzed. These systems have been tested in our thermal cycling test rigs at surface temperature 1100^{o}C. Influencing mechanical properties factors such as hardness and elastic modulus are systematically investigated. Further, the behavior of temperature gradient on the performance of thermal barrier coatings was also investigated.

1.3 Statement of Purpose

TBC is impacted by erosion, debonding effects and spallation, i.e. parts of the thermal insulation layer chip off, leaving the metal surface unprotected. A weakened turbine blade, rotating at 3000 or 3600 rpm carries the potential for severe consequential damage. Monitoring or predicting the TBC loss is important to avoid unscheduled engine failure or engine damage [4]. To further enhance the efficiency of gas turbines, next generation TBCs should possess higher temperature capability and a longer life time [1-7].

In applications of thermal barrier coating (TBC), partially stabilized zirconia (Zr) approaches some limits of performance. Current technology is based essentially on one thermal barrier material, 7YSZ. YSZ works quite well up to about 1200^{o}C. At higher temperatures, it undergoes microstructural changes and significant sintering which lead to a reduced life under thermal cyclic loading. The search for alternate materials has intensified in the recent past, affirmed primarily on the anticipation of substantially higher temperatures to improve the efficiency of gas turbines.

Major trends in novel compositions for reducing and/or stabilizing the thermal conductivity are based on pyrochlore-type based zirconates ($R_2Zr_2O_7$), a relatively new addition to the menu of TBC materials. Experimental evidence indicates that much remains to be done in this area to explore the advantages of rare earth zirconates such as high sintering resistance, no phase change up to its melting point and low thermal conductivity. Further investigation is required to examine the advantages of such functionally graded coating of these rare earth zirconates with YSZ at elevated temperatures.

The formulation of new coating materials GZ +YSZ as functionally graded TBCs are unique compared to existing TBC materials. In industrial gas turbines the turbine blades operate at 300^{o}C above the melting temperature of the alloy with the help of a very thin thermal insulation layer on the top of the super alloy called TBC and with tiny holes across the blade surface offering air passage for cooling the turbine blade from inside creating a temperature gradient across the super alloy metal substrate and the coated ceramic layer. Considering this fact providing a temperature gradient across the tested samples is considered as a very important feature during the thermal cycling tests for this thesis work. For these reasons, the results of thermal cycling with incorporating thermal gradient in this study are considered very important for scrutinizing functionally graded gadolinium zirconate as a promising material for next generation TBCs.

CHAPTER II

REVIEW OF LITERATURE

Development of the thermal barrier coatings started in 1950s and has been an attractive research area form many decades for the researchers. Research has been advancing in studying the adverse changes that occur due to thermo mechanical treatment of these different components-substrate, bond coat and top coat in hazardous environment of a gas turbine. This literature survey is focused on the prevailing TBC materials and the methods that are being used to study these materials. The survey also discusses some of the new trends in the area of Thermal barrier coatings TBCs.

2.1 Thermal Barrier Coatings (TBCs)

Thermal barrier coatings (TBCs) are coated on the components of the aircraft and industrial gas turbine engines to protect them from the most demanding high temperature environment and to improve the component durability [1]. Consolidation of TBCs system with internal cooling system of the turbine engines can reduce the surface temperature (100^{o}C to 300^{o}C) of the super alloy allowing an increase of the turbine inlet temperatures thereby increasing engine efficiency and performance [1]. Firstly TBCs are adopted to enhance the durability of metallic components in the hostile engine environment; coatings are now envisaged as prime-reliant elements in design, essential to extend the performance limits of current alloys as well as to enable the utilization of ceramics in gas turbines [2, 3].

Basic requirements while choosing the appropriate TBC's are 1.High melting point, 2. No phase transformation between room temperature and operation temperature, 3.Low thermal conductivity (<2.5 $W.m^{-1}.K^{-1}$), 4.Chemical inertness to the combustion gases and environment, 5. Reduced thermal expansion mismatch with the metallic substrate (> $10x10^{-6}K^{-1}$), 6. Good adherence to the metallic substrate and 7.Low sintering rate of the porous microstructure [4, 5].

Understanding the failure mechanism of specific TBC under its relevant engine operation conditions is very important to predict the life of the TBCs accurately [1].An accurate life prediction gives us the knowledge to use mechanism based methods in engineering practice [1].

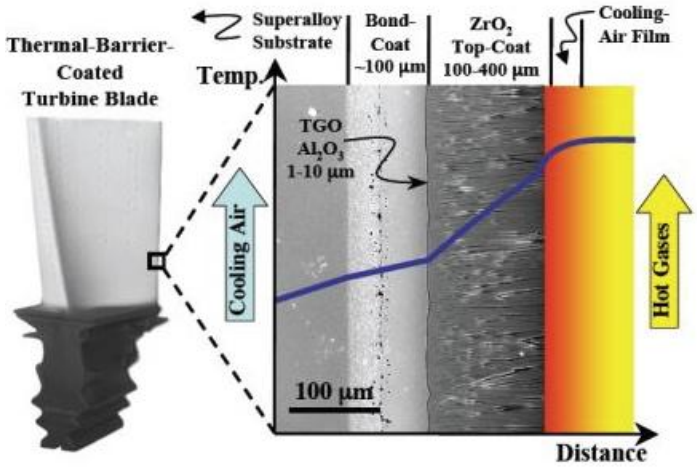

Figure 2.1 Schematic of a turbine blade illustrating the individual layers of a modern TBC system and an overlay of the temperature gradient in a high temperature environment. (Padture *et al.*, Science, [1])

2.1.1 Yttria Stabilized Zirconia (YSZ)

The initial zirconia-yttria TBCs contained from 12 to 20% of yttria, which was added to fully stabilize the cubic phase. Later, Stecura et al (1978) showed that better performance could be achieved by lowering the yttria level to between 6 to 8% [3]. Since there are coating durability and weight penalties associated with thicker coatings, turbine section ceramic coatings are typically limited to between 0.0127 and 0.0254 cm (0.005 and 0.010 in) [6].

YSZ is a state-of-art top coat material for TBC applications. YSZ shows excellent characteristics up to 1200^{o}C. At higher temperatures YSZ undergoes two major adverse changes. Significant sintering leads to microstructural changes and, hence, a reduction of the strain tolerance in combination with an increase of Young's modulus. Higher stresses originating in the coating will lead to a reduced life in-service performance. In the as sprayed YSZ coatings at elevated temperatures t′-phase transforms in to tetragonal and cubic phase. During cooling the tetragonal phase will further transform in to monoclinic phase, due to which the volume changes. As a result thermal cycling life is decreased [7].

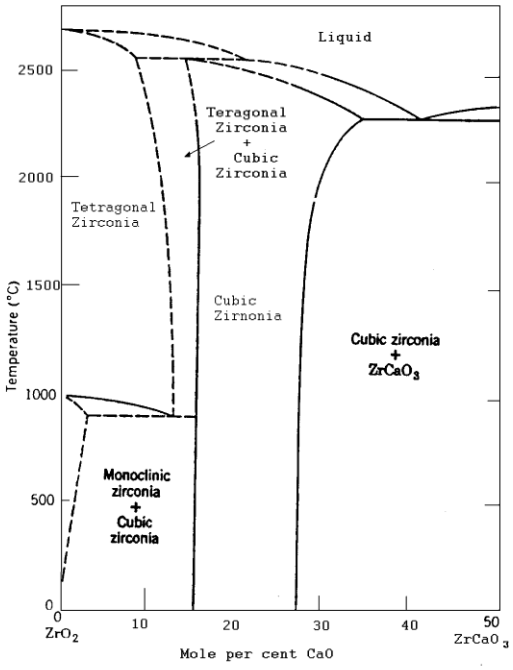

Figure 2.2 Phase diagram of Zirconia, (http://www.stanfordmaterials.com/zr.html)

2.2 Spraying Techniques

Key trends arise from the disparate attributes of electron beam-physical vapor deposition (EB-PVD) and atmospheric plasma spraying (APS) coatings, the former offering greater durability and the later better insulation efficiency [3].

A typical Air plasma spray (APS) coating is 300-600 µm thick. APS compared to EB-PVD coatings, involves low production costs and can handle larger sized material parts. APS TBCs are widely used for the bucket (blade) and nozzle (vane) applications in the gas turbines because of lowering operating temperatures and reduced temperature

gradients. Inner-"splat" grain morphology, cracks parallel to the metal/ceramic interface for low thermal conductivity, 15 to 20% porosity for low elastic modulus and low thermal conductivity are some of the favorable microstructure characteristics of APS coatings [1].

Typical APS and EB-PVD coated microstructures of processed samples are shown in Figure 2.3

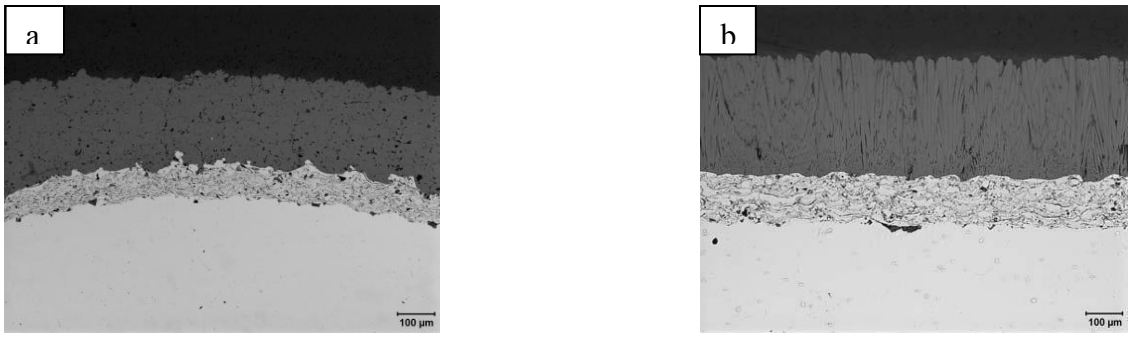

Figure 2.3 (a): APS thermal barrier coating, (b) EB-PVD thermal barrier coating

2.2.1Failure Mechanism in APS coatings

There are four failure mechanism involved in APS coatings.

(I)Stresses at the bond coat/ thermally grown oxide (TGO) interface are tensile at the crests and compressive at the troughs. Tensile stresses increases as the TGO increases which initiates a crack at the crests.

(II)Stresses at the top coat/ TGO interface are tensile at the crests and compressive at the troughs. Tension causes cracks at the crests.

(III)Due to the brittle nature of the top coat, cracks are initiated near the crests of the top coat/ TGO interface.

(IV)As the TGO thickens after a certain thickness the coefficient of thermal expansion of TGO/ bond coat composite becomes lower than that of the top coat and the bond coat which reverses the stress from compression to tensile at the troughs which causes cracks in the valleys of the top coat.

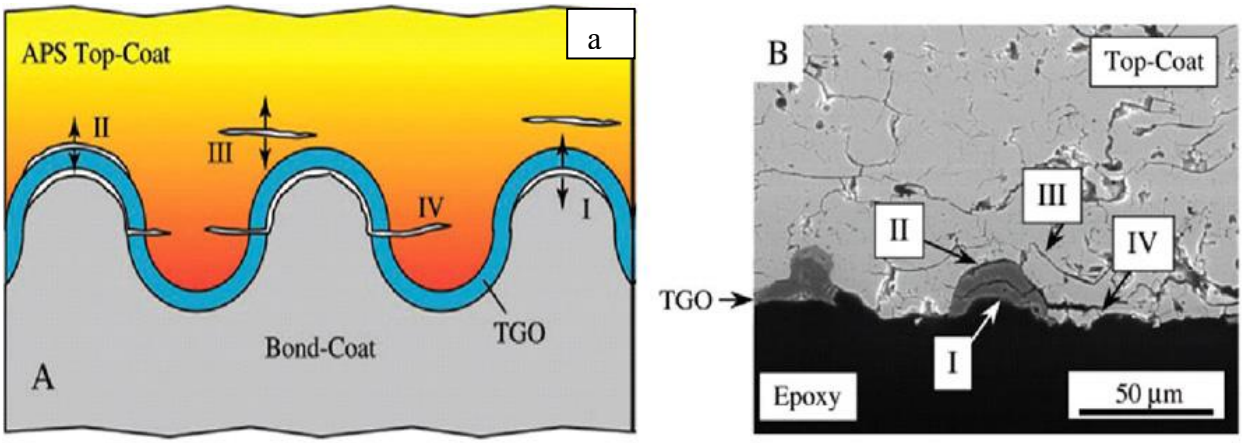

Figure 2.4 (a) Schematic diagram showing the four different cracking mechanisms in APS TBC. (b) Cross-sectional SEM of a failed APS TBC (240 cycles) mounted in epoxy showing the various cracking mechanisms illustrated in (a), (Padture *et al.*, Science, [1])

2.2.2Advantages of APS coating

APS applied coatings have low thermal conductivity than that of EB-PVD applied coatings. The coatings produced by APS typically have a thermal conductivity of 0.9~1.1 W/mK at room temperature due to the micro-cracks and the high volume fraction of inter-splat pores that are predominantly aligned parallel to the coating surface. The coatings applied using EB-PVD have a thermal conductivity in the range of 1.3~2.0 W/mK [8].

2.3 Gadolinium Zirconate (GZ)

Rare earth is a unitive term of 17 chemical elements including La, Ce, Pr, Nd, Pm, Sm, Eu, Gd, Tb, Dy, Ho, Er, Tm, Yb, Lu, Y and Sc.

Compounds of $A_2B_2O_7$ represent rare earth zirconates with pyrochlore structure. One possible crystal structure for $R_2Zr_2O_7$ (R=rare earth) is the light rare earths (La-Gd). $Gd_2Zr_2O_7$ has a very low thermal conductivity. Zirconate ceramics offer the advantage of having no phase transition during thermal aging and can maintain lower thermal conductivity than YSZ [9-11]. Below 1100^{o}C, the reaction between $Gd_2Zr_2O_7$ and Al_2O_3 is very slow [5].

An integrated gasification combustion cycle (IGCC) using domestically abundant coal to create rich H_2- rich synthesis gas as fuel is the future recommendation for generating electricity with gas-turbine engines [11]. It has been discovered that GZ TBCs are resistant to attack by molten calcium-magnesium-alumino-silicate (CMAS).

Experiments show that molten ash is arrested after penetrating ~25% of the TBC thickness which proves GZ is resistant to molten fly ash deposits in syngas-fired IGCC engines [12].

The thermo-chemical interaction between gadolinium zirconate ($Gd_2Zr_2O_7$) TBCs deposited by EB-PVD and a simulated CMAS melt (33Cao-9Mgo-13Ak$O_{1.5}$-45SiO_2 with a melting temperature of ~1240^oC) was investigated after isothermal exposure for 4h at 1300^oC by T.Steinke et al (2010). The study concluded that an approximately 6µm thick reaction layer was formed, which primarily consisted of a highly stable apatite phase based on $Gd_8Ca_2(SiO_4)_6O_2$ and fluorite ZrO_2 with Gd and Ca in a solid solution. The melt infiltration into the intercolumnar gaps of the EB-PVD coating rarely exceeded 30µm below the original surface. Future penetration was prevented by the crystalline reaction products filling the gaps. Due to details of the reaction, it was assumed that other rare-earth zirconates may behave similarly [13].

Due to the smaller thermal expansion coefficient ($9x10^{-6}K^{-1}$-$10x10^{-6}K^{-1}$) and lower fracture toughness (1.8 $MPa.m^{1/2}$-2.1 $MPa.m^{1/2}$) thermal cycling life of pure GZ coatings was much shorter than YSZ. However rare earth zirconates have many advantages such as high sintering resistance, no phase change up to its melting point and low thermal conductivity [5].

In a research done by Z.Xu et al. it was found that relatively low thermal expansion coefficient leads to high thermal stresses between the lanthanum-zirconium-

cerium composite oxide ($La_2(Zr_{0.7}Ce_{0.3})_2O_7$,$LZ_7C_3$) coatings and the metallic bond coat. The premature failure of the single LZ_7C_3 coatings can be mainly related to the chemical incompatibility of LZ_7C_3 coatings and TGO layer and its sharp decrease of thermal expansion coefficient at low temperature ($6.59 \times 10^{-6}K^{-1}$, 538K) might be the reason for the single layer LZ_7C_3 TBCs for the shorter thermal cycling life when compared to YSZ. It was suggested that to overcome this problem YSZ coating can be used as an interlayer between the new TBC material and the bond coat [14].

2.4 Multi-Layer Concept

Multi layer concept seems to be effective for the improvement of the thermal shock life of the TBCs. A multi layer includes an erosion resistant layer as the outer layer, a thermal barrier layer, a corrosion- oxidation resistant layer, a thermal stress control layer and a diffusion resistant layer [5]. In many recent TBC studies it has been reported that in a double layered TBC the top ceramic layer having a low thermal conductivity, high sintering resistance, and high phase stability acts as a thermal insulator to protect the inner ceramic layer.YSZ is usually used as a second ceramic layer which has high fracture toughness and large thermal expansion coefficient.

A double layered concept can not only increase the thermal shock resistance but also increase the application temperature of TBCs above 1250^{o}C [5].

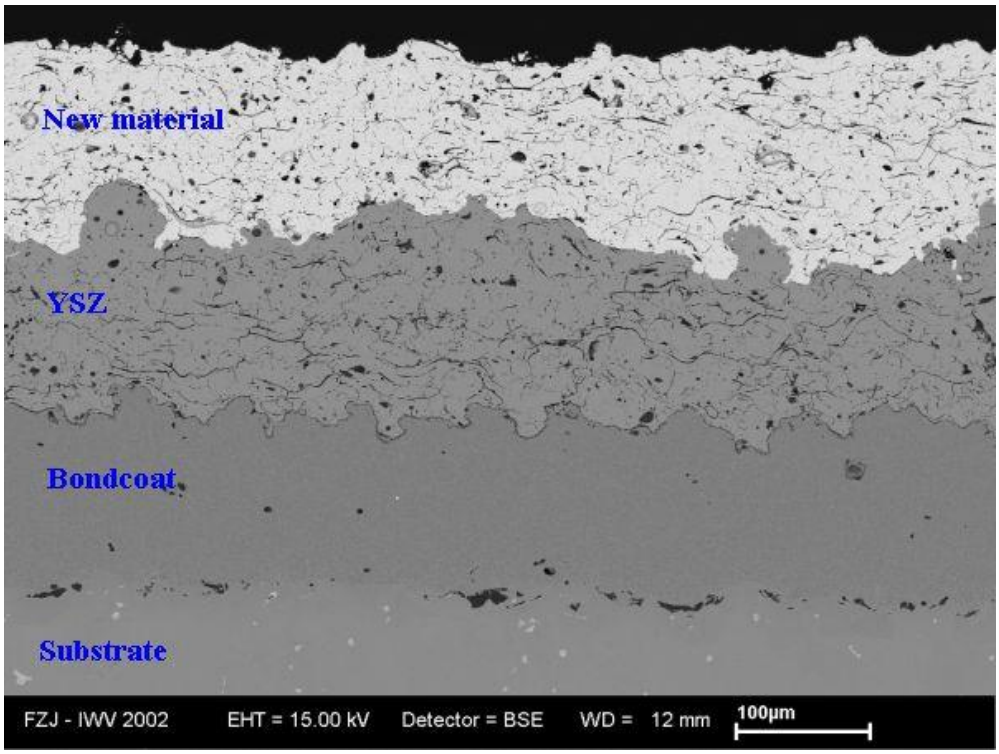

Figure 2.5 Schematic of the double layer TBC system illustrating various layers, (Vassen *et al.*, Journal of Thermal Spray Tech, [2])

In YSZ TBCs the spallation occurs at the interface of the top coat and the bond coat because of the chemical reaction between the top coat and the as-formed TGO layer. In the case of the double ceramic layer the spallation occurs at interface of the top ceramic layer and the bottom ceramic layer or inside of the YSZ bottom layer. It was quoted by Xu et al, [14] that at higher temperature YSZ layer could shrink and form micro cracks. The degradation could increase the Young's modulus which in turn decreases the tolerance against differing thermal expansion coefficient of YSZ layer and bond coat, and

then lead to a peeling of the YSZ layer. It was considered that when the compressive stresses are built up so much that become larger than the combination force of the LZ_7C_3/YSZ coatings' interface during thermal cycling, the spallation will occur not only at the interface between the LZ_7C_3 and YSZ layers, but also in the interior of the $LZ_7C_3$and YSZ layers[12]. Double layer made of perovskites fail at the bondcoat interface indicating that the failure is probably oxidation driven and not by limited temperature capability [13]. An investigation on the thermo-physical properties and high-temperature performances of TBC coatings is necessary in order to explore the possibilities of a potential TBC material.

2.5 Thermo Mechanical TBC Testing

In a study on GZ it was confirmed that when YSZ was added to GZ the thermal and elastic properties are improved when compared to pure GZ. Mechanical properties such as the hardness, stress-strain curve and load penetration curve measurements by indentation tests are evaluated. Phase analysis tests on YSZ doped GZ showed that the material has thermally stable pyrochlore structure. The reason for the enhanced mechanical properties such as hardness and elastic properties in the YSZ doped GZ compared to pure GZ mainly is because of the micro structural change that resulted from change in the densification behavior. The results show that the hardness was improved from 6 GPa to 10 GPa as measured by Vickers test and more than 20 GPa as measured by nano-indentation test with the addition of 3.52 wt% Y_2O_3 (4.56 mol% of YSZ to GZ) to GZ [13].

2.5.1Thermal Conductivity

The intrinsic thermal conductivity of ceramic coatings has an inverse dependence on the temperature according to the thermal conductivity theory. However from past studies it seems that thermal conductivities tend to increase with temperature for zirconia-based ceramics. This increase in the thermal conductivities at high temperatures was attributed to thermal radiation since the TBC materials are partially or fully transparent to thermal radiation at typical engine operating temperatures. Thus, to increase the thermal insulation capability of TBCs, both thermal conduction and thermal radiation must be considered [6, 15-16].

Maloney et al. reports a thermal conductivity of ~1.3 W. $(m.K)^{-1}$ (at $700^{o}C$) for a monolithic $Gd_2Zr_2O_7$ (fluorite phase) of unknown density, while a temperature-independent thermal conductivity of ~1.0 W. $(m.K)^{-1}$ is reported for a porous $Gd_2Zr_2O_7$ EB-PVD TBC [4].

Thermal conductivity is measured using laser-flash method. In a study it was reported that the thermal conductivity of 7YSZ decreases from ~3 W. $(m.K)^{-1}$ to ~2.3 W. $(m.K)^{-1}$ over the temperature range of 25^{o}-$700^{o}C$ [4].

The two factors that may contribute to lower thermal conductivity of GZ when compared to 7YSZ are (i) the significantly higher concentration of oxygen vacancies present in this material, as a result of 33 mol% Gd_2O_3 addition, and (ii) the effective phonon scattering by gadolinium solute cations as a result of the significant atomic-

weight difference between gadolinium (157) and Zirconium (91). In the case of 7YSZ the addition of 7wt% (5.8 mol %) yattria decreases the conductivity of 7YSZ significantly from its pure zirconia upper bond because of the introduction of oxygen vacancies [12]. Thermal conductivities of the pyrochlore and the fluorite materials are identical; the ordering in the pyrochlore structure does not appear to have any effect on the phonon-scattering cross section relative to the fluorite structure [4, 17].

2.5.2 Coefficient of Thermal Expansion

Thermo mechanical compatibility with the under lying alumina should be a primary requirement of any top coat material, since and reaction that consumes the TGO would likely replace it with a less protective oxide [2]. In studies by H.Zhou et al. (2007) it was found that linear coefficient of thermal expansion of CeO_2 doped Lanthanum zirconate ($La_2Zr_2O_7$, LZ) is higher than 8YSZ for temperatures over 400^oC. It was considered that thermal expansion coefficient of LZ can be evaluated by adding CeO_2. Thermal expansion coefficient of GZ is 8.1~10.5 x $10^{-6}K^{-1}$at 200~1000^oC [8].

2.5.3 Mechanical Properties

The mechanical properties such as the elastic modulus and hardness are measured by nano-indentation. Nano-Indentation tests on YSZ TBCs showed that the elastic modulus of the TGO was considerably higher when compared to the bond coat and the top coat. Such large differences in the elastic modulus could lead to severe thermal stresses near the TGO, which may be the reason why the failure of the TBC by thermal fatigue usually occurs at or near the TGO [18, 19]. It was reported that as aging time

increased, the sintering of the top coat material occurred and the elastic modulus of the top coat increased as a result of the sintering effect. In a study, the elastic modulus and the nano hardness of the YSZ top coat increased at an aging time of 100h as compared to the as-sprayed properties, and then remained almost constant afterwards. The study inferred that the sintering was active as to lead to an increase of the elastic modulus and nano hardness up to 100h, and that there was no further sintering after 100h, because the top coat was already fully saturated [19-22].

2.6 Thermal Cycling

Life of TBC system was essentially dependent on the thermal profile of the engine. Typical cycles in aircraft engines are 1h cycles (45-50 min at elevated temperature and 15-10 min of forced air cooling) between 1080^0C and room temperature or 1135^0C and room temperature. For internal gas turbine applications with their extended dwell at elevated temperatures, typically 24 h cycles (23 h at elevated temperature with 1h of forced air cooling) at 1080 or 1121^0C are used [20]. Failure criterion was typically 20% spallation of the TBC surface. During thermal cycling due to the mismatch of the thermal expansion coefficient between the ceramic and the bond coat, stress accumulation results at the TBC/bond coat interface. This was the most critical area of the TBC/bond coat system, due to the abrupt change in mechanical and physical properties [23-25].

There are different testing methods used to determine the failure mechanism of TBCs. Some of the testing methods are (i) The Furnace cycling test (FCT) which creates

a high- temperature isothermal environment for enhanced bond coat oxidation with a moderate thermal shock to cyclically stress the ceramic/bond coat interface. A sample id exposed for a long time to elevated temperatures, which leads to significant bond coat oxidation. However, the TBC temperature during soaking was too low to cause pronounced sintering in the ceramic [23]. (ii) The jet engine thermal shock test (JETS) which creates a large thermal gradient (several hundred degrees Celsius) across the TBC. Due to the large thermal gradient through the ceramic, the TBC/bond coat interface oxidizes only marginally. (iii) Fluidized bed test (FBT) in which test samples are transported to the hot zone of the test rig which consists of a standard fluidized bed furnace. The test samples are transported back to the cold zone in which compressed air is directed onto the TBC surface [23].

Bolcavage et al, [23] compared these three test methods using different TBC samples ranging from spray dried and sintered 7-9 YSZ powders, double layered TBC system with different ceramic compositions, dense vertically cracked APS and EB-PVD TBC. It was determined that the FCT test reflects the actual engine condition well because it not only cyclically stresses the TBC but also degrades the bond coat through severe oxidation. It also reveals performance and design limits such as bond coat depletion. At high temperatures sintering occurs in the top coat resulting in partial healing of the cracks and reaction in porosity which will increases the thermal conductivity and reduces the strain tolerance of the top coat [1]. In order to assess sintering behavior in a two layer TBC, it is important to first understand the sintering behavior of its constituents.

However it does not really address TBC degradation caused by defects in the ceramic layer, such as crack propagation or sintering, which typically initiate above 1300^0C. It is suitable for performance ranking of the complete TBC system emphasizing the bondcoat / TBC interface [23-26].

Cooling the TBC to room temperature by air and water quenching are two popular methods for cooling the TBCs while testing under thermal cycling. Investigation suggests that the extremely rapid cooling associated with water quenching can mask the zirconia destabilization which was clearly evident in the more realistic thermal cycling conditions involving air cooling, there by resulting in a questionable ranking of materials [12].

2.7 Current status and Summary

Some of the earlier studies in our research group have analyzed the behavior of YSZ top coats of selected APS and EB-PVD microstructured coatings for their thermal mechanical behavior and thermal properties characterization. Agu et al. studied the effect of coating properties of ZrO_2 and Al_2O_3 multilayer composite coatings on failure of TBCs. In his work it was observed that the thermal conductivity tent to reduce with increasing value of Al_2O_3 ratio in the composite coating mixture. Silava et al. studied the microstructure effect on the thermo-physical properties of YSZ TBCs. Polasa et al. studied the mechanical properties of YSZ and Al_2O_3 multilayer composite coatings in addition to high temperature oxidation and hot corrosion of multilayer TBCs [27-30]. In his work it was observed that addition of hafnium to NiCoCrAlY bond coats reduced the activation energy of the growth process which could increase the further oxidation. Nono

indentation testes on the hot corrosion tested multilayer thermal barrier coatings showed that hardness and youngs modulus values are higher in multilayer thermal barrier coatings processed with higher percentage of alumina in the coatings. The selection of the test matrix and design of the experiments for this thesis work have inspirations from the previous work that was carried out in our research team.

Literature review indicates that no much work has been done in investigating the role of GZ powders in thermal cycling behavior of thermal barrier coatings. It is also very essential to study the mechanical properties in order to understand the mechanical integrity of these TBC systems.

There is also a need in the prior art for a test rig that can reproduce the conditions such as high temperature, temperature gradient, high pressure, erosion, corrosion, and thermal and mechanical loading, that occur in an operating gas turbine engine.

CHAPTER III

EXPERIMENTAL METHODOLOGY

As discussed in the introduction chapter, the main objective of this thesis is to investigate and analyze the thermal cycling life and mechanical properties of functionally graded GZ+ YSZ TBCs in addition to single layer GZ and YSZ TBCs. This current chapter systematically discusses the various experimental methodology used to accomplish the thermal cycling tests, porosity tests and measurement of influencing mechanical properties such as hardness and elastic modulus. This chapter also discusses in detail about the Novel temperature gradient thermal cycling furnace that was fabricated in our facility, LSU, Baton Rouge to study the behavior of temperature gradient on the performance of thermal barrier coatings.

3.1 Sample Fabrication

A group of specimens in this work are prepared using APS Standard (STD) coating type by a third party, Material Solution International (MSI) at Houston TX. Another group of samples are prepared using our in-house plasma spraying (Sulzer-Metco 9M, Winerhur, Switzerland) equipment. A SG-100 air plasma spray gun with internal powder feed injection at MSI was used for the spraying through the instrumentality of a FANUC 710i robot, a precision of the spray equipment that ensured precise gun to-part motion and repeatability of the process. Operation parameters, such as spray distance, arc current, voltage, flow rate, carrier gas flow rate, the gun speed,

powder feed rate, chamber pressure and nozzle diameter etc are carefully monitored during the sample preparation process. This thesis does not present detailed information about the process for proprietary reasons.

The bond coat and top coat powder compositions used for the preparation of these samples are presented in the following Table 3.1

Table 3.1 Composition (by weight) of powders for APS spray

Powder details		Content by Weight (%)									
Coating Type	Material	Ni	Co	Cr	Al	Y	ZrO2	Y_2O_3	Si	Hf	Gd_2O_3
Bond Coat 1	NiCoCrAlY	Bal	22	17	12.5	-	-	0.6	0.4	0.25	-
Bond Coat 2	NiCrAlY	Bal	-	21.88	9.85	0.85	-	-	-	-	-
Top Coat 1	YSZ	-	-	-	-	-	Bal	7.65		-	
Top Coat 2	GZ						Bal				59.5

The bond coat and the top coat powders are sprayed on disc shaped (IN) 738 superalloy substrate material of 0.5inch (12.7mm) in diameter and 0.125inch (3.175mm) in thickness. Disks are grit blasted with alumina and ultrasonically cleaned in acetone for 1 hour before APS coating. Two types of coatings are prepared: for single layered TBCs ~300µm/600µm thick YSZ and GZ are applied on to the bond coat; for double layered TBCs after coating the bond coat with the pure YSZ (~150µm/300µm in thickness), a mixture of x%wt GZ and (100-x)%wt YSZ (~150µm/300µm in thickness) is applied as the top layer.

The schematic of the coating construction of the four layers of the TBC samples discussed and the function of each individual layer is presented in the Figure 3.1.

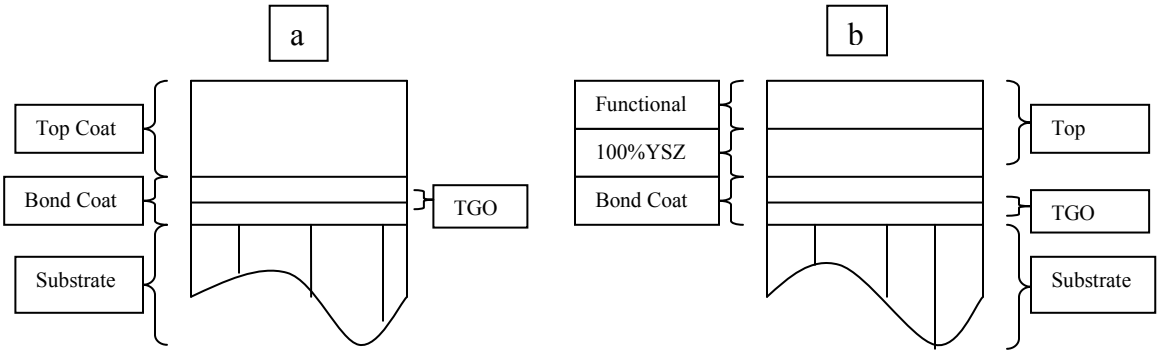

Figure 3.1 Schematic of coating construction of different components of (a) Single layer and (b) Double layer TBC Systems

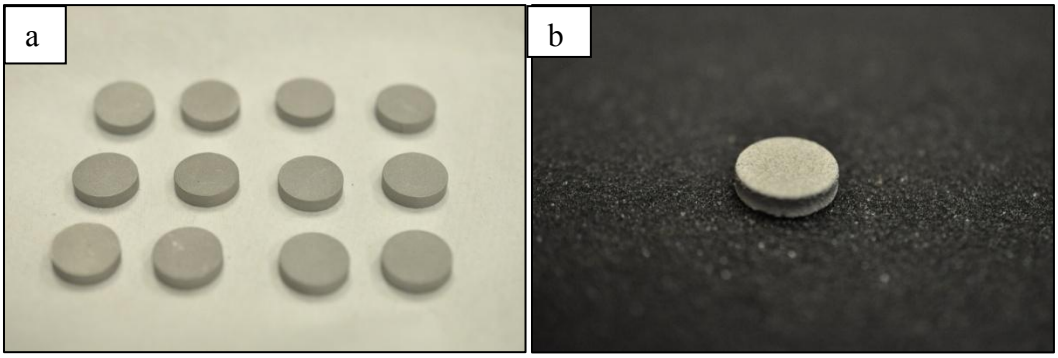

Figure 3.2 (a) Disc shaped (IN) 738 superalloy substrate material, (b) TBC sample after APS spraying

The porosity and Nano Indentation tests are conducted on the 600µm thick ceramic top coat samples (Table 3.2) and isothermal cycling tests are conducted on the 300µm thick ceramic top coat samples (Table 3.3). Temperature gradient thermal cycling tests are conducted on the 300µm thick ceramic top coat samples (Table 3.4). Details of all test specimens are given under in Tables 3.2, 3.3 and 3.4

Table3.2 Test Matrix for Nano Indentation and Porosity Tests

	Substrate	Bond Coat	TBC	No of Samples	Coating Type
1	IN 738	NiCoCrAlY+Hf 120µm	7wt%YSZ SPECIMENS	2	STD APS (600 µm)YSZ dense 100% YSZ top layer
2	IN 738	NiCoCrAlY+Hf 120µm	GZ SPECIMENS	2	STD APS GZ(600 µm) dense 100% GZ top layer
3	IN 738	NiCoCrAlY+Hf 120µm	STD APS COATINGS AS SPECIFIED IN COATING TYPE	2	STD APS YSZ dense bottom layer (300 µm) + 75% YSZ & 25% GZ top layer (300µm)
4	IN 738	NiCoCrAlY+Hf 120µm	STD APS COATINGS AS SPECIFIED IN COATING TYPE	2	STD APS YSZ dense bottom layer (300 µm) + 50% YSZ & 50% GZ top layer (300µm)
5	IN 738	NiCoCrAlY+Hf 120µm	STD APS COATINGS AS SPECIFIED IN COATING TYPE	2	STD APS YSZ dense bottom layer (300 µm) + 25% YSZ & 75% GZ top layer (300µm)

Table 3.3 Test Matrix for Isothermal Thermal Cycling Tests

	Substrate	Bond Coat	TBC	No of Samples	Coating Type
1	IN 738	NiCoCrAlY+Hf 120µm	7wt%YSZ SPECIMENS 300 µm	3	STD APS YSZ dense 100% YSZ top layer
2	IN 738	NiCrAlY 120µm	GZ SPECIMENS 300 µm	3	STD APS GZ dense 100% GZ top layer
3	IN 738	NiCoCrAlY+Hf 120µm	STD APS COATINGS AS SPECIFIED IN COATING TYPE	3	STD APS YSZ dense bottom layer (150 µm) + 90% YSZ & 10% GZ top layer (150µm)
4	IN 738	NiCoCrAlY+Hf 120µm	STD APS COATINGS AS SPECIFIED IN COATING TYPE	3	STD APS YSZ dense bottom layer (150 µm) + 75% YSZ & 25% GZ top layer (150µm)

Table 3.4 Test Matrix for Thermal Gradient Thermal Cycling Tests

	Substrate	Bond Coat	TBC	No of Samples	Coating Type
1	IN 738	NiCrAlY 120µm	7wt%YSZ SPECIMENS 300 µm	3	STD APS YSZ dense 100% YSZ top layer
2	IN 738	NiCrAlY 120µm	GZ SPECIMENS 300 µm	3	STD APS GZ dense 100% GZ top layer
3	IN 738	NiCrAlY 120µm	STD APS COATINGS AS SPECIFIED IN COATING TYPE	3	STD APS YSZ dense bottom layer (150 µm) + 50% YSZ & 50% GZ top layer (150µm)

3.2 Porosity Measurement Tests

Porosity measurement tests are conducted using Poremaster-33 analyzer; a porosimeter manufactured by Quantachrome Instruments is used to measure the total porosity of the specimens as shown in Figure 3.3.

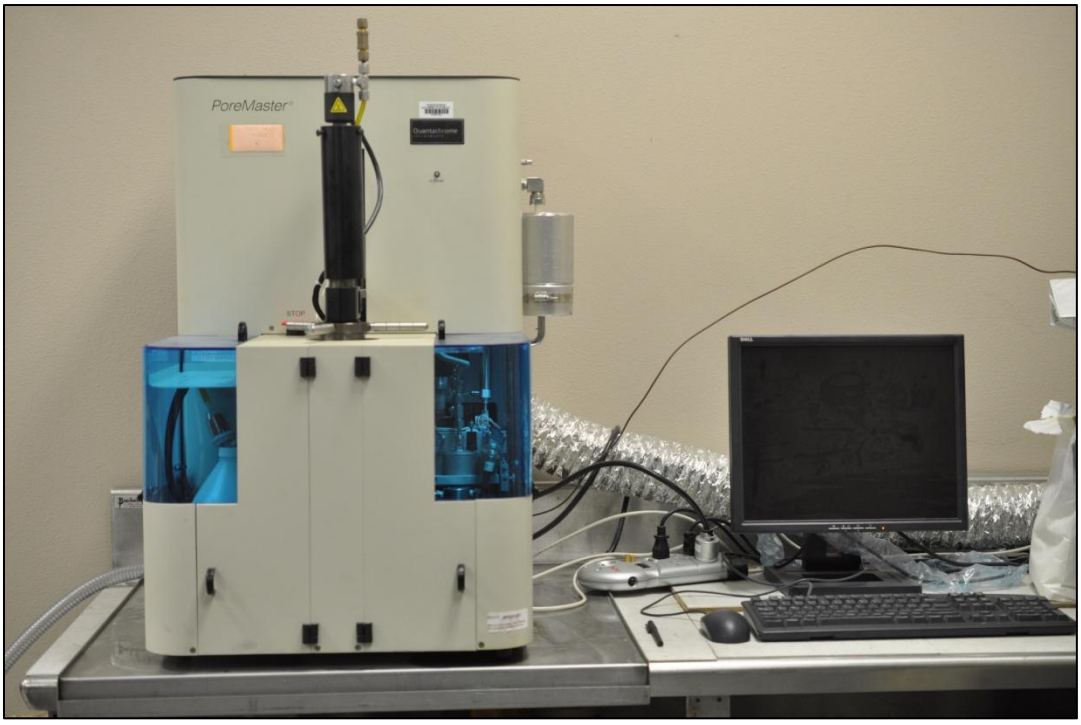

Figure 3.3 Poremaster-33 for Mercury Intrusion porosity testing

Method

The voids in a material are filled with another probe material, either gas (helium or nitrogen) or a liquid (mercury or water) by method called intrusion porosimetry. Potentially, the probe material's volume is measured as a function of the filling pressure, Ilavsky, (2009). The instruments ability to calculate the porosity values is based on

mercury intrusion porosimetry which involves the intrusion of a non-wetting fluid (mercury) into the specimen's void by increasing the fluid pressure up to 33,000 psi. This instrument is capable of measuring the total volume of mercury intruded into the sample and the bulk volume of the sample using the following equation (Poremaster-33 equipment manual, 2006-2007):

$$\text{Porosity (\%)} = \frac{V_t}{V_b} x100$$

Where V_t is the total volume of mercury intruded and V_b is the bulk volume of the sample.

Sample Preparation

Porosimetry experiments require free standing samples of a top coat separated from the substrate specimen. To accomplish this concentrated hydrochloric acid (HCl) solution of about 98% concentration is used. The samples that are to be separated are placed in individual 50ml glass beakers before introducing the acid and placed under the working hood. Approximately 20-25 ml concentrated HCl is introduced in to the beakers with the samples. The beakers with the samples and the acid are left to stand about 24hours to achieve good separation inside the hood. After 24 hours, the samples are removed with a wooden spatula in to another beaker containing Ethyl Alcohol, rinsed for 10 minutes on ultrasonic cleanser to make sure no concentrated HCl particulates are left in the pores of the ceramic coating. The cleaned samples are dried in a furnace at 200^{o}C for 5 minutes to make sure that Ethyl Alcohol is evaporated.

3.3 Mechanical Properties Measurement Tests

Mechanical properties measurement tests are conducted on TI-900 TriboIndenter manufactured by Hysitron Incorporated is used to perform the nano indentation tests on the specimens as shown in Figure 3.4.

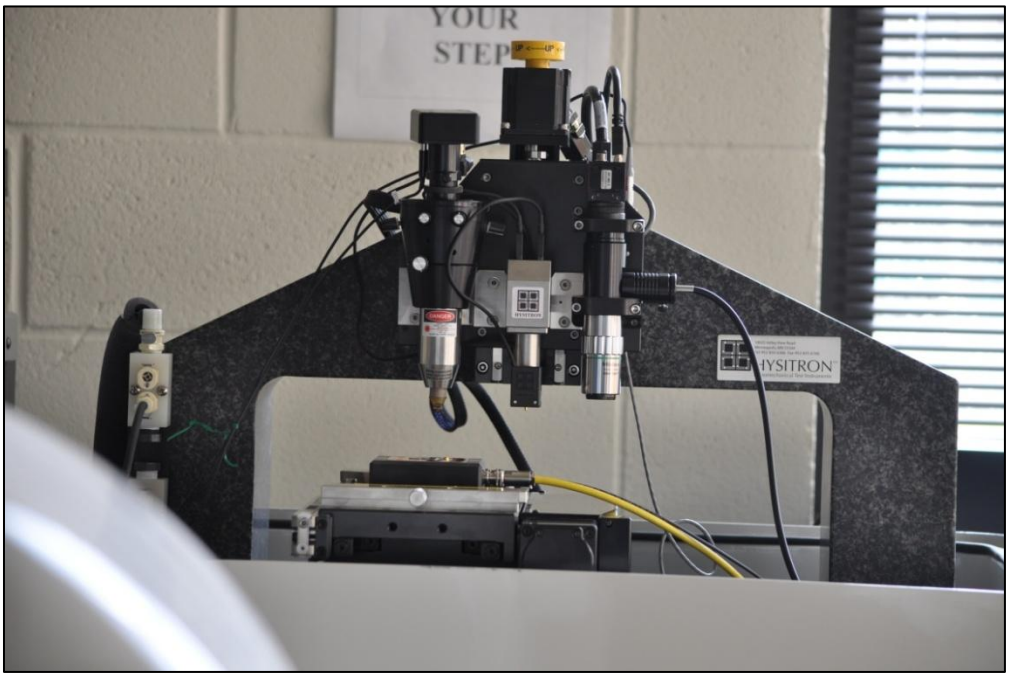

Figure 3.4 TI-900 TriboIndenter for Nano Indentation tests

Method:

Standard quasi-static regime testing is done using the standard TriboIndenter. A 3-segment Quasi-Static load function with respect to force and time is chosen considering the begin force, end force and segment time, and test indentation is performed on the

polished cross section specimens. The Berkovich probe with a half-angle of 65.35^{o} and radius of curvature of approximately 150nm is used to indent the specimen (Figure 3.5).

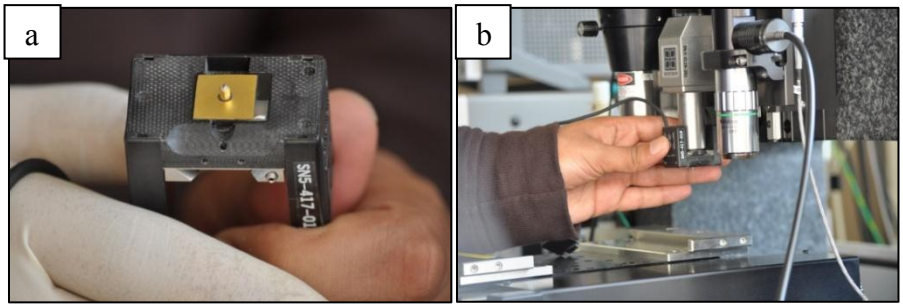

Figure 3.5 (a) Berkovich probe, (b) optical micro scope and nano indenter setup

Indentation is performed across the samples cross section starting from the ceramic top layer and followed by the bond coat and finally on the substrate at a regular range. With the top-down optics feature, micro scale features of the sample are tested directly from the optics window. Specimens are imaged using in-situ imaging to reveal nano scale features and indents are placed with nm accuracy.

Data Analysis

After the indentation is completed a quasi-static indentation file with load vs. displacement cure will pop up. Clicking the execute fit button in the lower right corner will calculate the reduced modulus and hardness from the load vs. displacement curve. The following procedure is used to calculate the hardness and reduced modulus E_r and calculated Young's modulus E_c.

1. The contact depth, h_c is calculated with equation

$$h_c=h_{max}\text{-}0.75x\ \frac{P_{max}}{S}$$

Where H_{max} is the maximum depth and P_{max} is the maximum applied force and S is the stiffness

2. The hardness is calculated with equation

$$H=\frac{P_{max}}{A(h_c)}$$

Where P max is the maximum applied force and A is the projected contact area

3. The reduced modulus is calculated with equation

$$E_r=\frac{\sqrt{\pi}}{2\sqrt{A(h_c)}}x\ S$$

Where A is the contact area h_c is the contact depth and S is the stiffness.

4. The Young's modulus is calculated with equation

$$E_c=(1\text{-}V_c^2)\ x[\frac{1}{E_r}-\frac{(1-V_i)^2}{E_i}]$$

Where E_i and V_i are the Young's modulus and the Poisson's ratio of the indenter and E_c and V_c are for the material and E_r is the reduced modulus calculated by the computer from the indentation files.

Sample Preparation:

Nano Indentation require cross sectioned and polished samples for indentation. To acquire this encapsulation of a sample with a resin is required. This method will preserve the original microstructure and distribution of components and edges in the sample by

immersion of the sample within a resin in a mold to improve the external integrity of brittle materials. After the epoxy samples are prepared the samples are cut in to two pieces using diamond cutter at a moderate rpm and feed rate so that a smooth surfaces are attained. After acquiring the cross sectioned samples the samples are polished with polishing papers and alumina powder solution (Figure 3.6).

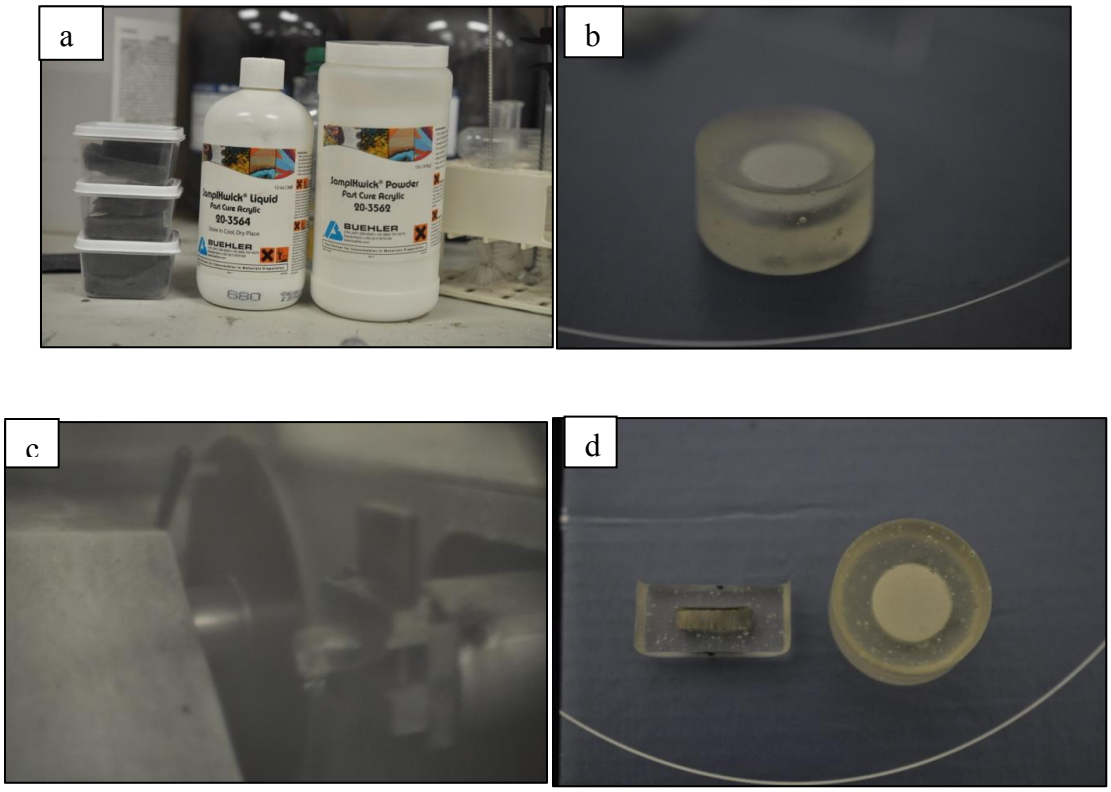

Figure 3.6 (a) Samplkwick Acrylic used for encapsulation, (b) Encapsulated TBC sample, (c) Diamond cutting blade for achieving the cross sectioned samples, (d) Cross sectioned sample

3.4 Isothermal Cycling Tests

Isothermal cycling tests are conducted using CM 1700 bottom-loading programmable furnace equipped with a 2404 control set point program as shown in Figure 3.7.

Figure 3.7 CM 1800 bottom loading programmable furnace for isothermal cycling tests.

Method

The furnace is programmed for a "ramp up-dwell-ramp down" cyclic operation. In Each cycle the furnace is heated (ramp up) from room temperature to 1100^{o}C in 30 min (ramping rate: 36^{o}C/min) and isothermally soaked (dwell) at 1100^{o}C for 60 minutes following cooling (ramp down) to room temperature in 15 minutes (ramping rate: 73^{o}C/min) as shown in Figure 3.8

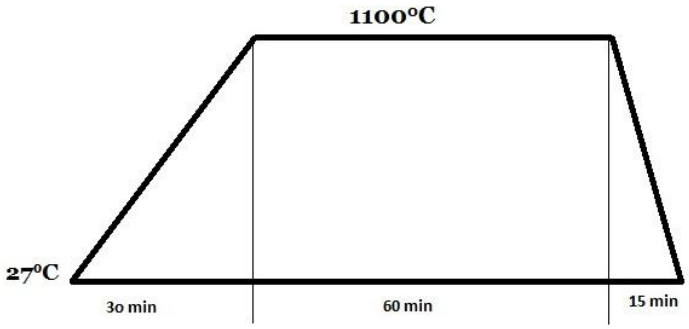

Figure 3.8 Schematic of the temperature profile used for isothermal thermal cycling tests on CM Furnace.

Basic Operation

After switching on the power the controller will run through a self-test sequence for about 3 seconds and then shows the Home display consisting of measure temperature in the upper readout and target set point in the lower readout. The controller is programmed to Automatic mode in which the output is automatically adjusted to maintain the temperature or process value at the set point.

A flow chart for the basic operation of CM 1700 bottom loading furnace is presented in figure 3.9. Augmentation of every command can be seen below the pictures.

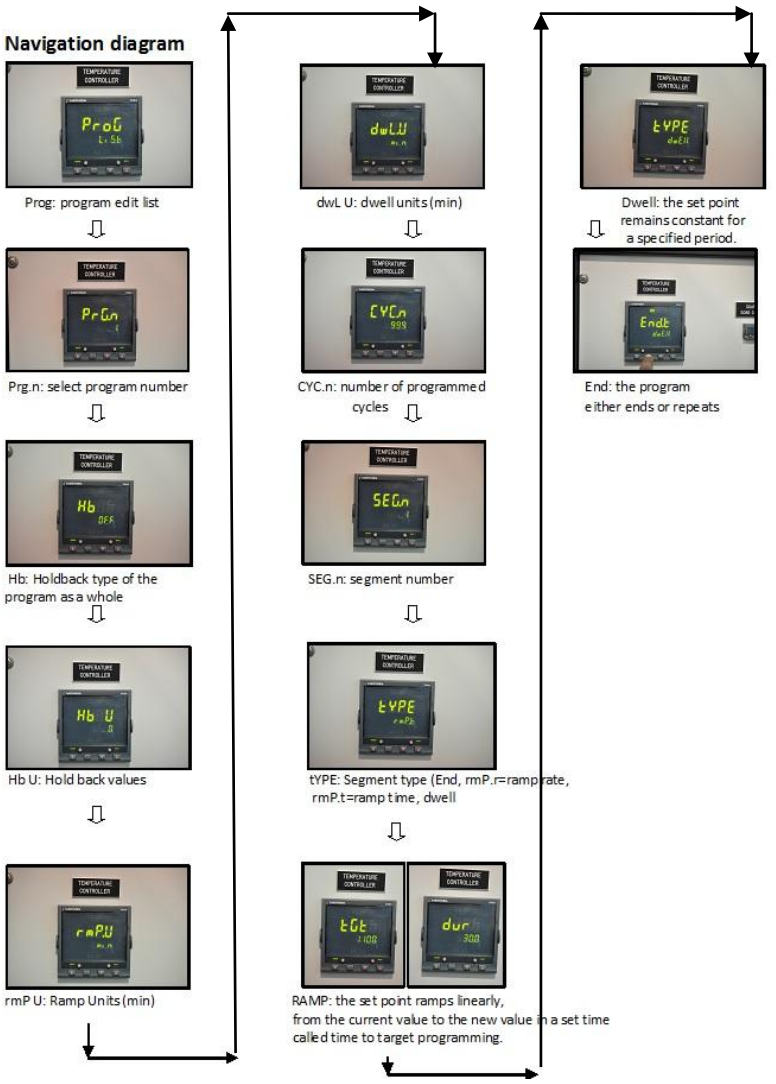

Figure 3.9 Flowchart of the basic operation of CM 1700 programmable furnace equipped with a 2404 control set point program

3.5 Temperature Gradient and Controlled Environment Furnace

Temperature gradient and controlled environment furnace is designed to test TBCs by mimicking the conditions inside of gas turbine providing a temperature gradient across the sample, cyclic operation, and mass flow system in a pressurized vessel as shown in Figure 3.10.

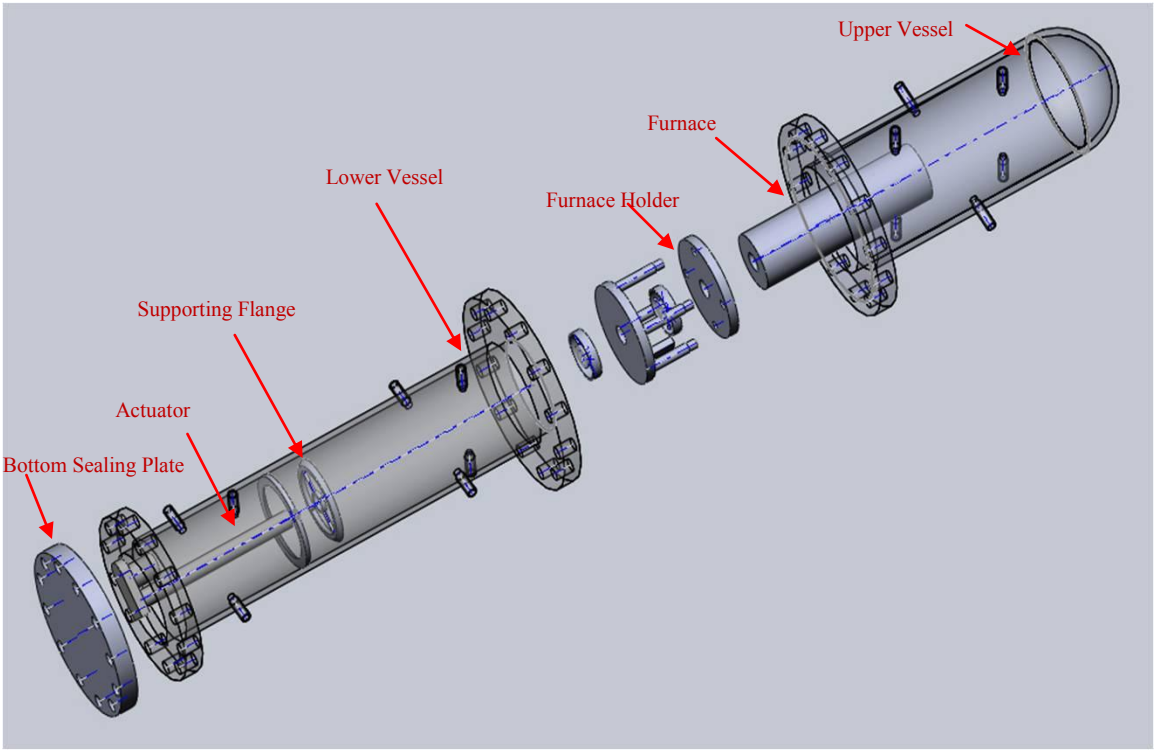

Figure 3.10 Schematic of the test rig for controlled temperature gradient and environment (~ ⌀ 20" x 84") designed in Solidworks 2010

Concept

The intention for developing Temperature gradient and controlled environment furnace test rig is to reproduce conditions such as high temperature, temperature gradient, high pressure and thermal loading that occur in an operating gas turbine engine. This apparatus can provide more detailed examining capabilities about the effect of the actual engine operating conditions in the existing gas turbine on the TBCs.

Features of the TBC Test Rig

A furnace heater with 2500 watts power capable of producing 1600^{o}C is used (Figure 3.11). A sample holder capable of creating a temperature gradient of ~200^{o}C across the sample and can perform cyclic operation to transport the sample from hot zone to cold zone periodically with the help of a Ball screw linear actuator is developed as shown in Figure 3.12 . An external vessel which can resist the heat dissipation of the heater and can create a pressurized environment and provide an isolated gas composition around the sample away from the ambient air is established. Figure illustrates the apparatus pressurized at 130 Psi. A mass flow system containing gas tanks (oxygen, nitrogen and carbon dioxide), tank regulators, tubing and fittings, mass flow controller and a relief and gas mixture manifold is acquired. Finally a 84.25 inches long Testing apparatus which can perform cyclic operation in a furnace heating environment providing a temperature gradient across the sample, a mass flow system to isolate the gas composition around the sample in a pressurize environment is actualized.

Figure 3.11 Thermal cycling experimental set up including furnace heater, temperature controller and furnace holder

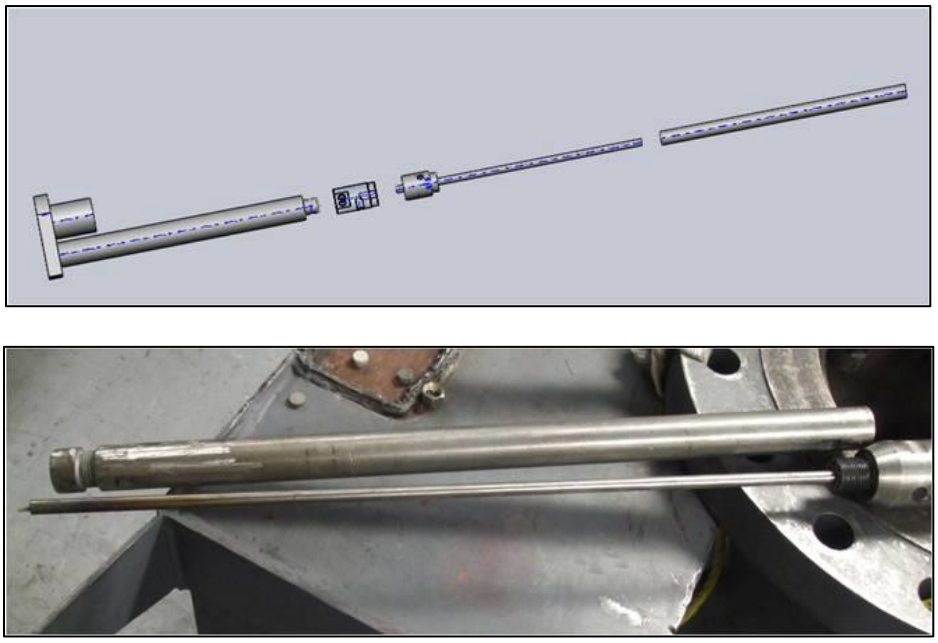

Figure 3.12 Key components of the sample holder mechanism

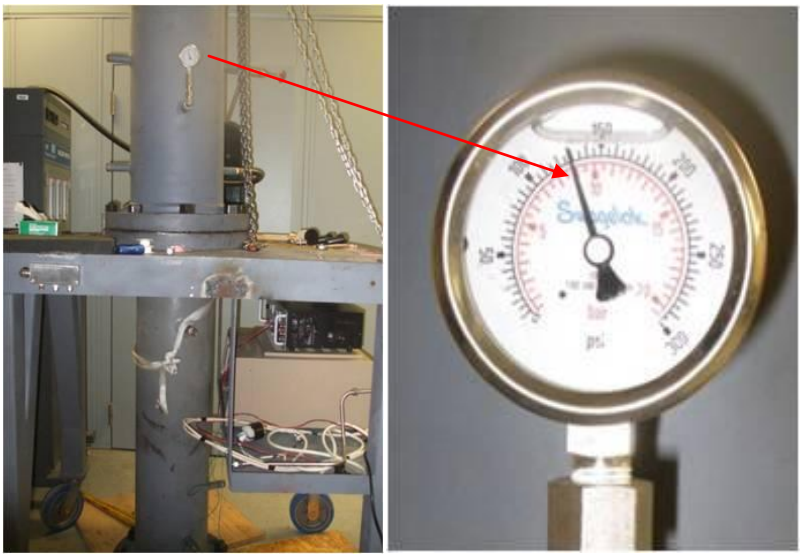

Figure 3.13 TBC test rig pressurized at 130 Psi

Concept of temperature gradient in detail

Turbine blades operate at 300^{o}C above the melting temperature of the alloy. The blades are coated with a very thin thermal insulation layer on the top of the super alloy called TBC and also tiny holes across the blade surface offering air passage for cooling the turbine blade from inside as shown in Figure 3.14 creating a temperature gradient across the super alloy metal and the coated ceramic layer. Considering this fact providing a temperature gradient across the tested samples is considered as a very important feature during the Thermal cycling tests for this thesis work.

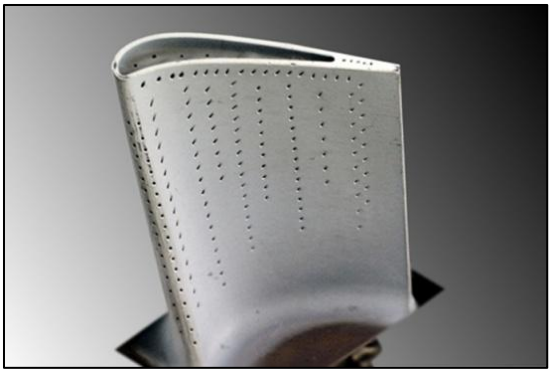

Figure 3.14 Turbine Blade with air vents and coated with TBC insulating system, Courtesy of: http://www.yxlon.com/Applications/Cast-parts/Turbine-blades

The temperature gradient across the sample is achieved by running compressed inside the sample holder assembly as shown in the Figure 3.15. An S type thermo couple is introduced in the sample holder assembly in such a way that it can measure the temperature of the bottom surface of the sample holder platform. It is assumed that the surface of the sample sitting on the sample holder platform will also have the same temperature the platform acquired (Figure3.16). The S type thermocouple is connected to omega temperature recorder which refreshes the temperature reading for every 4 seconds (Figure 3.17). From the preliminary tests it is confirmed that a temperature gradient of ~200^{o}C is achieved across the sample. Figure 3.18 illustrates the temperature profiles of the recorded temperatures for temperature gradient thermal cycling tests where furnace test temperature is at 1100^{o}C

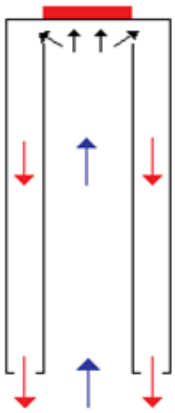

Figure 3.15 Compressed air flow mechanism

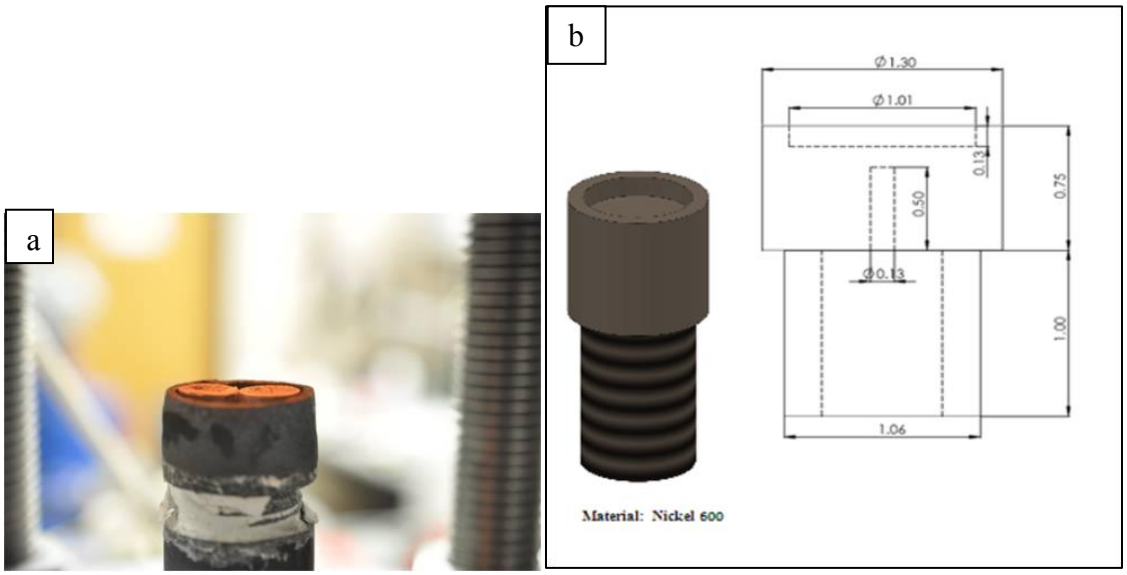

Figure 3.16 (a)Sample holder platform,(b)Schematic of the temperature gradient capability sample holder- solidworks

Figure 3.17 Omega Temperature Rocorder

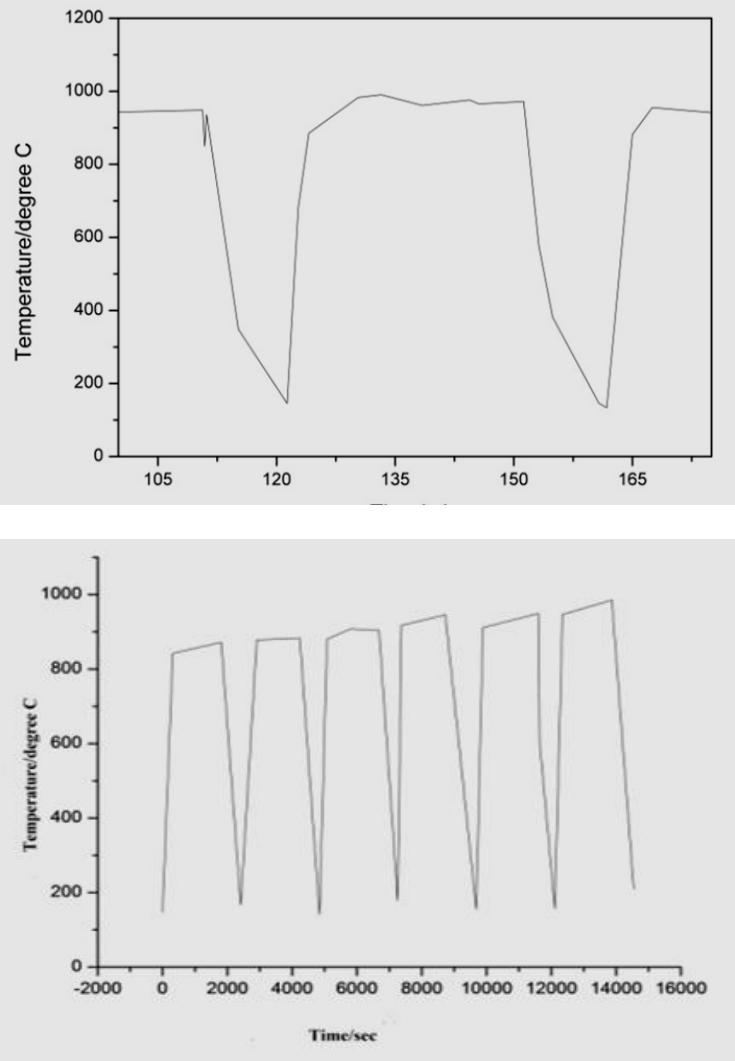

Figure 3.18 Temperature profile set up for experimental TBC thermal cycling.

(Furnace test temperature 1100^{o}C)

Temperatures Gradient Thermal Cycling Tests

Temperature gradient thermal cycling tests are conducted using above mentioned novel temperature gradient and controlled environment furnace. Tests are conducted at a furnace test temperature of 1100^{o}C along with a temperature gradient of ~200^{o}C. The

temperature program used for these tests and the key components of thermal loading mechanism are shown in Figure 3.19

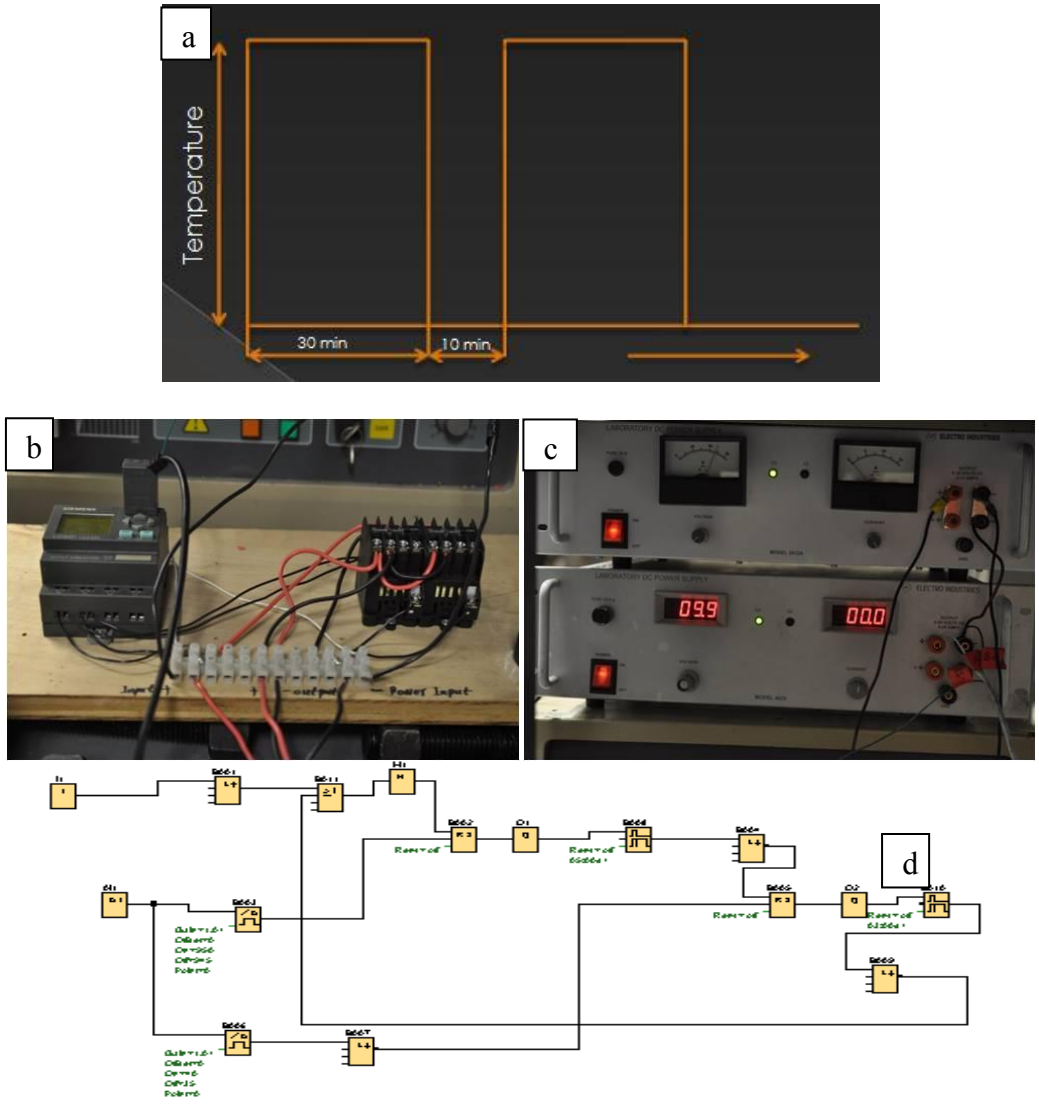

Figure 3.19 (a) Schematic of the temperature profile used for temperature gradient cycling tests, (b) (c) (d) components of the automated thermal loading mechanism

3.6 Scanning Electron Microscopy Evaluation

Scanning electron microscope from FEI is used to study the morphology of the different components of the TBC system- substrate, bond coat and top coat. The equipment is shown in Figure 3.20

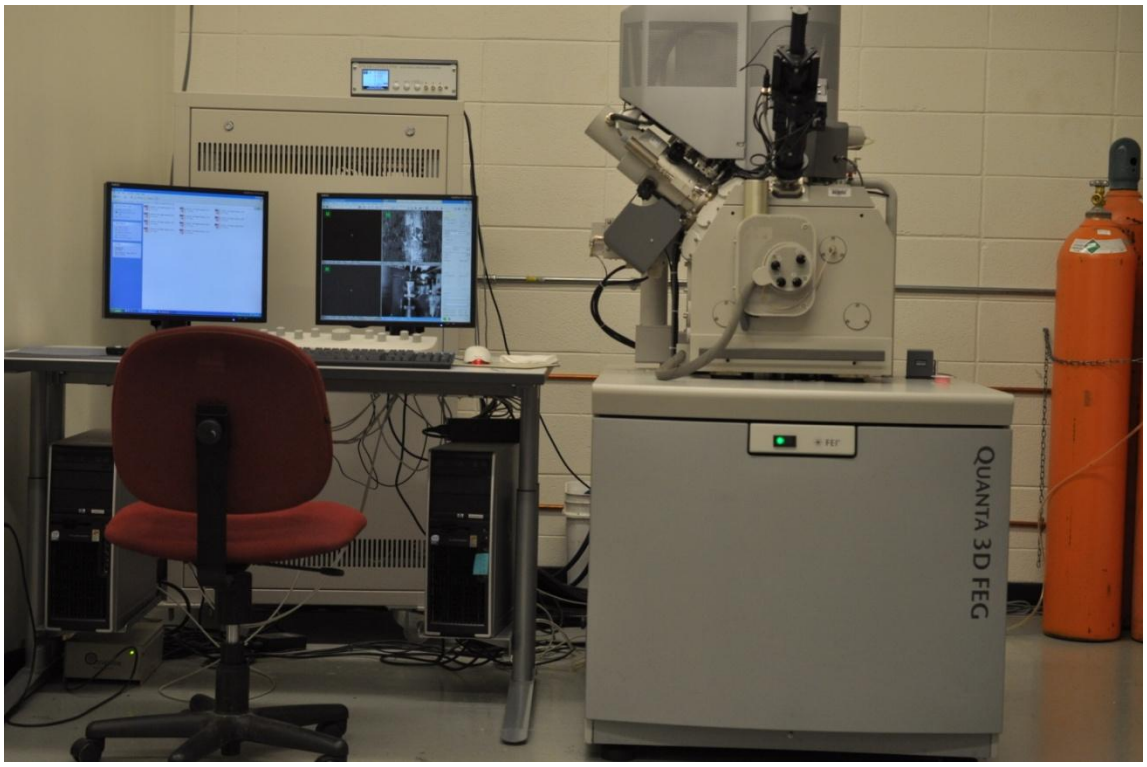

Figure 3.20 Quanta 3D FEG Scanning electron microscope for studying the morphology of the failed TBC samples

Method

The test samples foe SEM evaluation are introduced in to a vacuum chamber and with the help of the software interface the appropriate magnification and focus is selected and the failure of the TBC samples is carefully examined and pictures are saved for a later analysis.

Sample preparation

Samples are prepared in the similar fashion that has been described earlier in this chapter (see 3.3 Mechanical Properties Measurement Tests).The cross sectioned samples are coated with thin layer of platinum for achieving the clear images.

CHAPTER IV

RESULTS AND DISCUSSION

This current chapter systematically discusses the results of thermal cycling tests, porosity tests, mechanical property measurement and microstructural analysis tests, whose experimental methodology has been explained in chapter III. This chapter also discusses in detail about the various failure modes and structural changes that took place during the isothermal and temperature gradient thermal cycling testing with inference from literature where topcoat complete delamination, top coat segmentation cracking, failure within the top coat are reported.

4.1 Porosity test results

The porosity of the selected TBCs is characterized quantitatively by mercury intrusion porosimetry using Poremaster. All the samples are fabricated using APS-STD process. Porosity results for the tested samples are presented in Table 4.1 and plotted on Figure 4.1

Table 4.1 Density and Porosity values of different TBC systems tested

Sample	Density (Kg/m^3)	Porosity (%)
YSZ (600µm)	4795.6	18.1
GZ (600µm)	5860.9	22.4
DL 25%GZ /YSZ(600µm)	4555.1	23.5
DL 50%GZ/YSZ (600µm)	5612.7	25.8
DL 75%GZ/YSZ (600µm)	5202.1	20.3

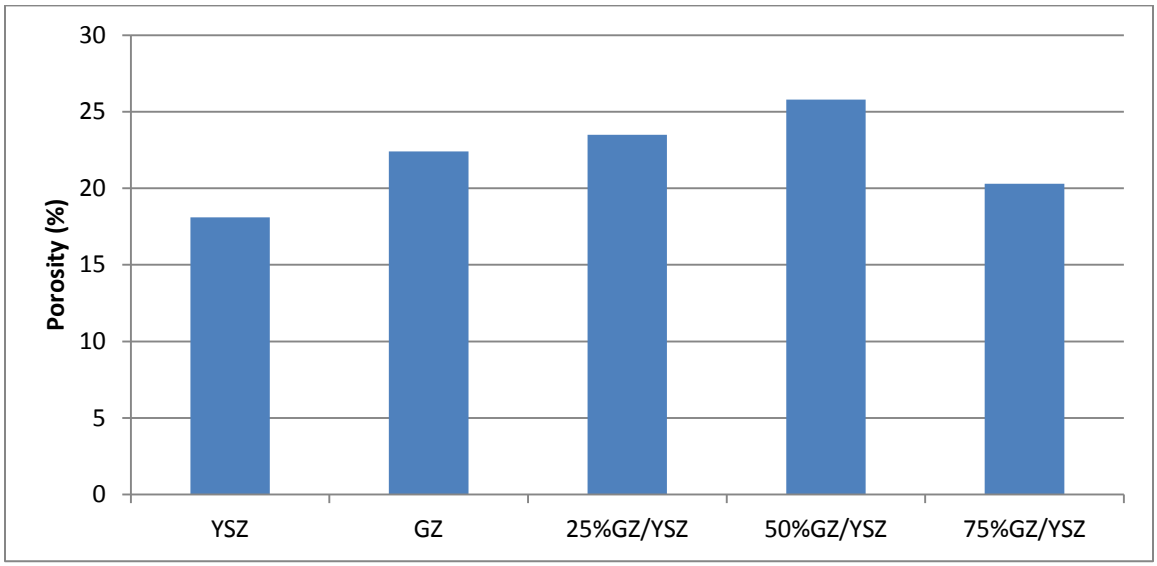

Figure 4.1 Porosity values of different TBC systems tested

Thermal conductivity of a TBC is greatly affected by the presence of porosity. Volume fraction V_v, of the pores in the TBCs that will decrease the net section area through which heat can be transported by phonons which in turn reduces the thermal conductivity. Increasing the porosity will reduce the thermal conductivity; however above certain values, this increase can degrade the mechanical integrity of the ceramics. From the results shown in table above, porosity of all the TBC systems are around 18% to 25%. Usually, a porosity of at least 12% is required for TBC to sustain good thermal barrier effect [20]. Porosity of thermal barrier coatings might be affected by deposition parameters like working distance and power of the plasma gun while spraying the ceramic powders during sample preparation process.

4.2 Mechanical Properties measurement results

Mechanical properties such as elastic modulus and hardness are measured by nano indentation on the cross-section of the coating specimens. YSZ, GZ and the functionally graded TBCs by adding GZ to YSZ in 25%, 50% and 75% ratios are being tested. Tests are conducted choosing a 3 segment Quasi-Static load function with respect to force and time considering the begin force, end force, segment time and indentation is performed on the polished cross section specimens. Each segment is 10seconds and peak indentation load is10, 000 μN.

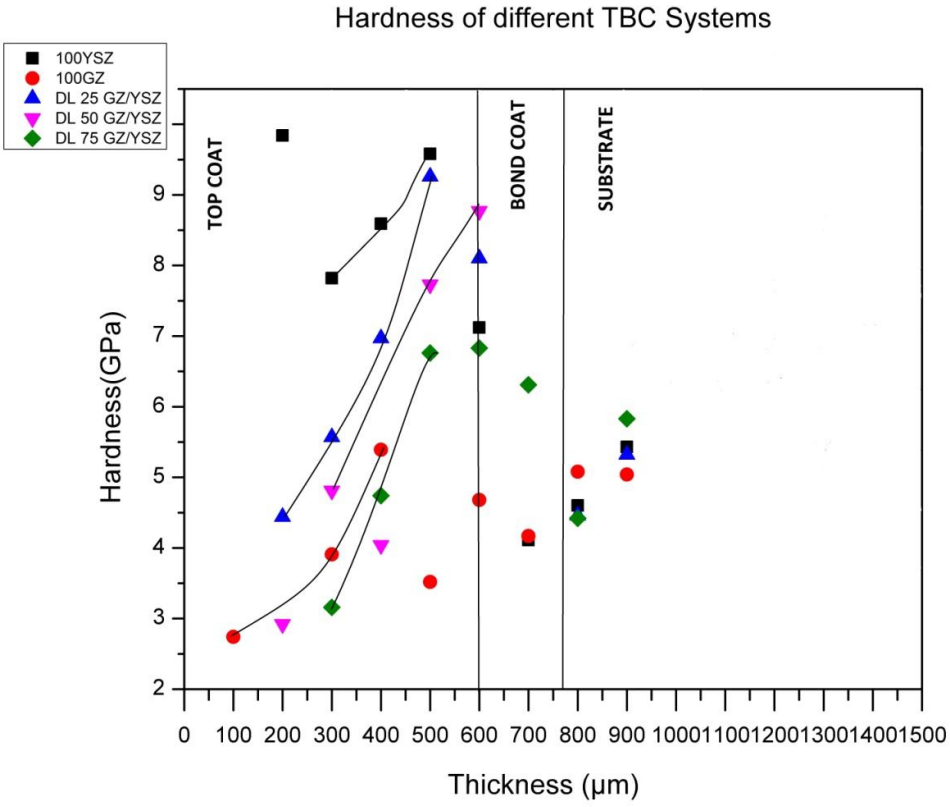

Figure 4.2 Hardness measurements of different TBC systems tested

Measured hardness and the elastic modulus of all the 5 TBC systems with respect to the thickness across the cross section of the sample have been presented in Figure 4.2 and Figure 4.3. Among the tested TBC systems YSZ has the high hardness while GZ has the lowest hardness. Note that the hardness of 25%GZ/YSZ and 50%GZ/YSZ double layered systems is greater than that of pure GZ TBCs. From the pattern followed by the tested TBC systems it is evident that the functional TBCs with decreasing GZ percentage improves the hardness of the TBC system, yet 25% GZ/YSZ double layer system doesn't show significant improvement when compared to 50%GZ/ YSZ double layered system. One reason would be the micro porosity beneath the indenter.

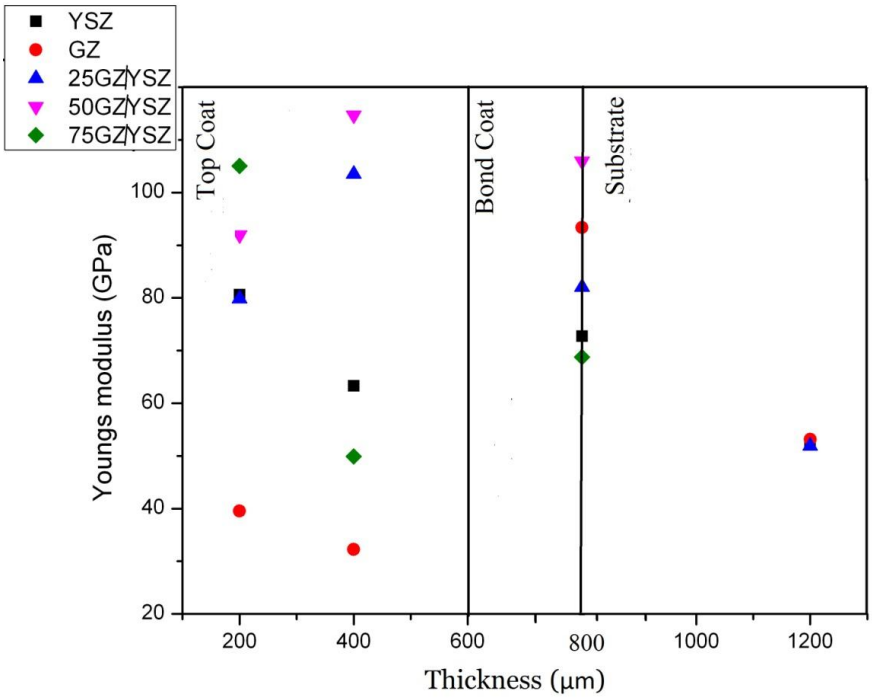

Figure 4.3 Young's modulus measurements of different TBC systems tested

Some of the variations of the Young's modulus and hardness values of the substrate and the bond coat are probably due to the presence of inter phase boundaries near the indent. It is expected that a higher elastic modulus and yield stresses would contribute to high resistance to damage from particle attacks or wear during gas turbine operation when the TBCs are not subjected to critical failure caused by TGO formation. It is also notable that porosity plays an important role in improving the mechanical properties (Table 4.1). As the hardness and Young's modulus of 50% GZ/YSZ DL layered system is similar to that of YSZ we can say that mechanical properties of GZ based functionally graded TBC system are expected to show superior thermal cycling life when compared to pure GZ TBCs while maintaining lower thermal conductivity than YSZ systems.

4.3 Results of Thermal Cycling Experiments

In the present section thermal cycling test results of isothermal cycling tests and temperature gradient thermal cycling tests are presented. All the samples used for isothermal cycling tests are fabricated using APS STD process by third party, Material Solution International (MSI) at Houston TX. All the tested samples are exposed to 1100^{o}C.

4.3.1 Isothermal cycling test results

Table 3.2 presents the specifications and Figure 4.4 presents the thermal cycling lives of the tested samples.

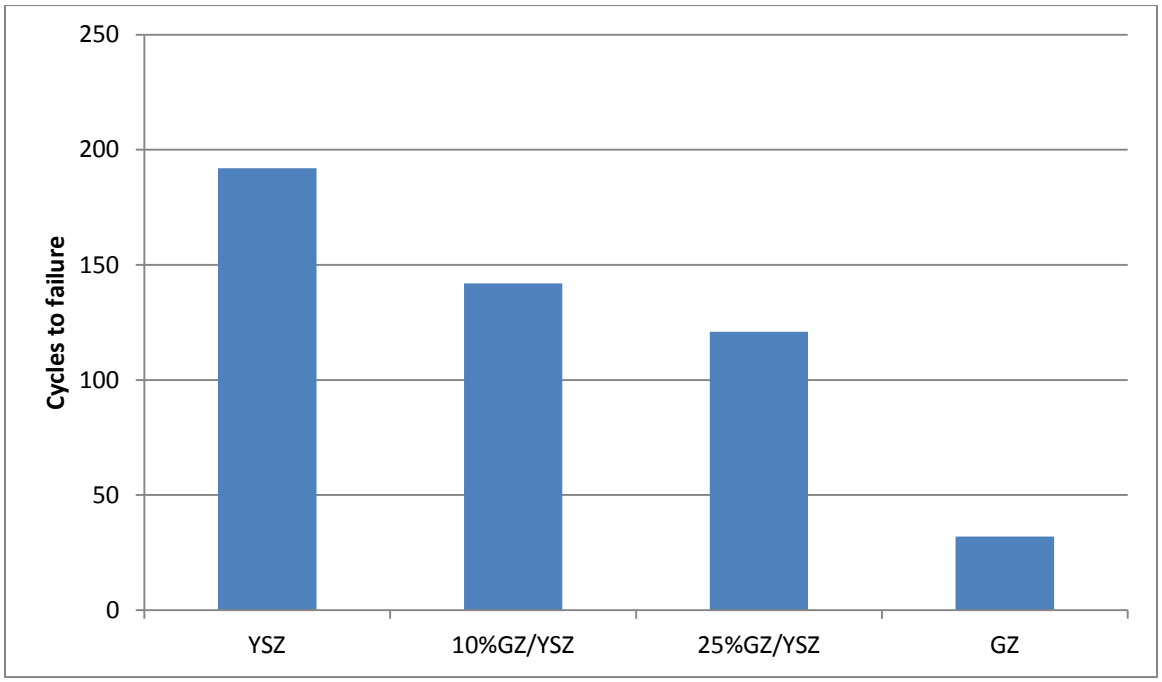

Figure 4.4 Thermal cycling lives of different TBC systems after Isothermal cycling tests carried at 1100^{o}C

On the 1.45-hour-cycle, upon exposure to 1100^{o}C, Only GZ showed visible failure after 22 cycles. The YSZ and DL 10% GZ and 25% GZ TBC Specimens showed promising thermal cycling life as can be deduced from the data in Figure 4.4. All the tested TBCs failed in the ceramic layer close to the interface between the ceramic layer and the TGO, leaving spots of ceramics on the surface of the bond coat, which is often occurred in APS coating systems. Another interesting phenomenon that should be noticed is that the ceramic layer often came off in a whole piece after thermal cycling tests

The failure of YSZ samples is mainly caused by the delamination initiation from the edge of the coupons. Pure GZ samples have the similar failure mechanism as YSZ samples. It can be clearly seen that the life time of pure GZ coatings is well below to those of standard YSZ coatings. Functionally graded double layer systems showed significantly higher life time when compared to pure GZ coatings. In double layer systems spallation location is likely to occur either at the interface between the functionally graded GZ/YSZ layer and the YSZ layers or inside the YSZ bottom layer. The degradation of the TBC could lead to an increase in Young's modulus of the coatings. The increase in the Young's modulus during thermal cycling is an indicator for the loss of tolerance against differing CTE of ceramic layer and bond coat which leads to a peeling off of the ceramic layer. The coefficient of thermal expansion mismatch either between GZ and YSZ layers or YSZ and TGO layers is regarded as one of the primary factors to influence the thermal cycling life of these double layer coatings.

In industrial gas turbines most coated components are actively cooled from the back side, resulting in a temperature gradient during operation. Moreover, during engine shut down, the coating surface can cool quite rapidly causing additional gradients. All the above tests are carried out in an air furnace under uniform temperature. This arrangement leads to the lack of temperature gradient in the samples in comparison to the actual engine conditions. More over in this kind of experiments severe oxidation occurs in the bond coat as the designed working temperature (~950^{o}C) of the bond coat is lower than the maximum temperature used for these tests (1100^{o}C) due to which the thermal cycling life of the TBCs is short. Yet the isothermal cycling tests help us for comparative study.

4.3.2 Temperature gradient thermal cycling test results

In this present experiment, a novel and unique test approach is used with thermal gradient incorporated in cycling testing. This approach is applied to create a more realistic loading situation, closer to actual engine conditions. The sample surface is cooled with compressed air to achieve the desired temperature gradient across the TBCs. This could make it easier to differentiate between different materials and coating properties and asses the applicability of the analyzed coatings closer to real operating conditions.

A thermal gradient cycling test combines severe and frequent cycling with the exposure to high impact temperature on the surface of the coating and active cooling of the substrate (at the back) and further will include thermal shock by active cooling of the surface at the end of each cycle. Thus a thermal gradient test will be representative of real

operation conditions in power generation gas turbines, where high cycling and even higher temperature will occur due to short term demand of energy and higher efficiency needs.

The tests are stopped when significant failure is detectable. Such failure is typically defined by spallation/delamination of the coating covering more than 20% of the sample surface area.

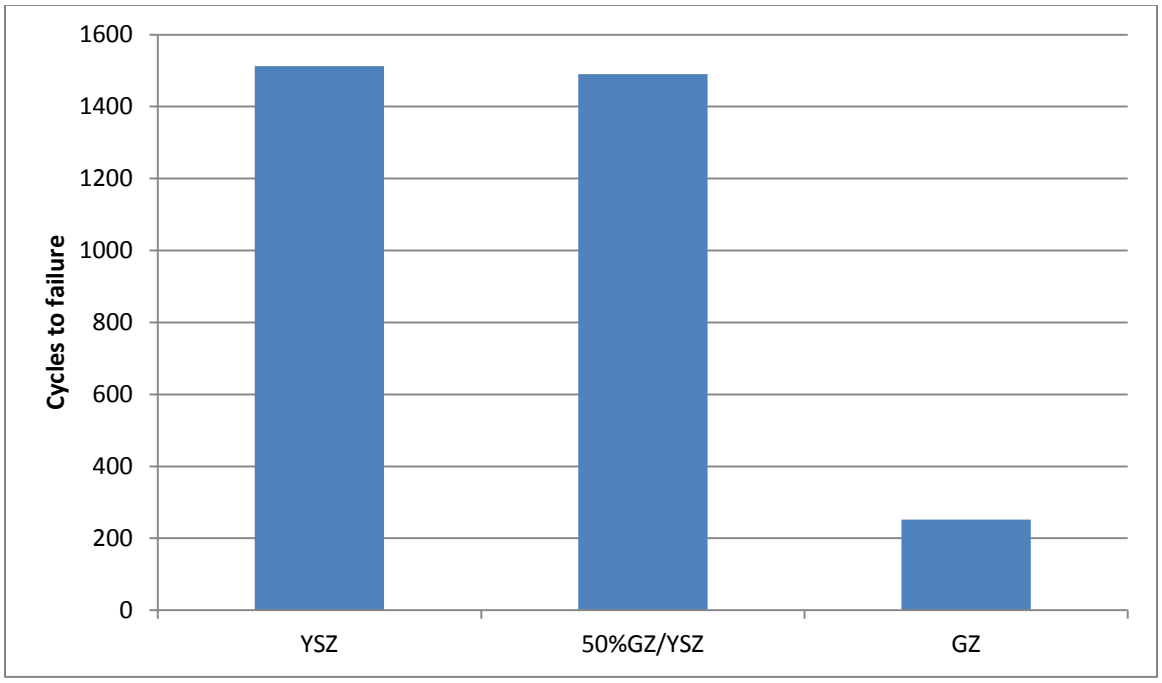

Figure 4.5 Thermal cycling results of temperature gradient thermal cycling tests carried out in the TBC test Rig at 1100°C

From results shown in Figure 4.5, on 40 minutes thermal cycle incorporated with thermal gradient up on exposure to 1100^{o}C, only pure GZ samples showed visible failure after 200 cycles. YSZ and functionally graded double layer 50%GZ/YSZ didn't show any symptoms of failure till 1500 cycles. One major reason for these improved thermal cycling would be temperature gradient. As the exposed temperature of the bond coat exposed is similar to the designed working temperature of the bond coat (~950^{o}C) which can be correlated to the lower growth rate of the thermal grown oxide at these temperatures. From Figure 4.6 it can be clearly seen that in both the YSZ and double layer 50% GZ/ YSZ samples the failure is mainly caused by the spallation at the edges.

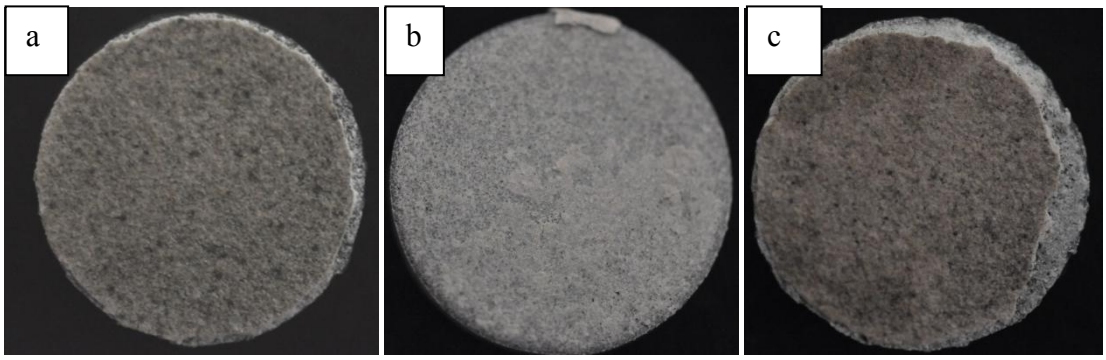

Figure 4.6 (a) YSZ, (b) GZ, (c) 50%GZ/YSZ failed TBC samples after thermal gradient thermal cycling tests

At moderate surface temperatures the functionally graded double layer 50%GZ/ YSZ TBC system meets the expectations, as the thermal cycling performance is similar to those of YSZ TBCs.

4.4 Microstructural Analysis

The cross sectioned SEM images of the TBC samples after thermal cycling testes are presented in Figure 4.7

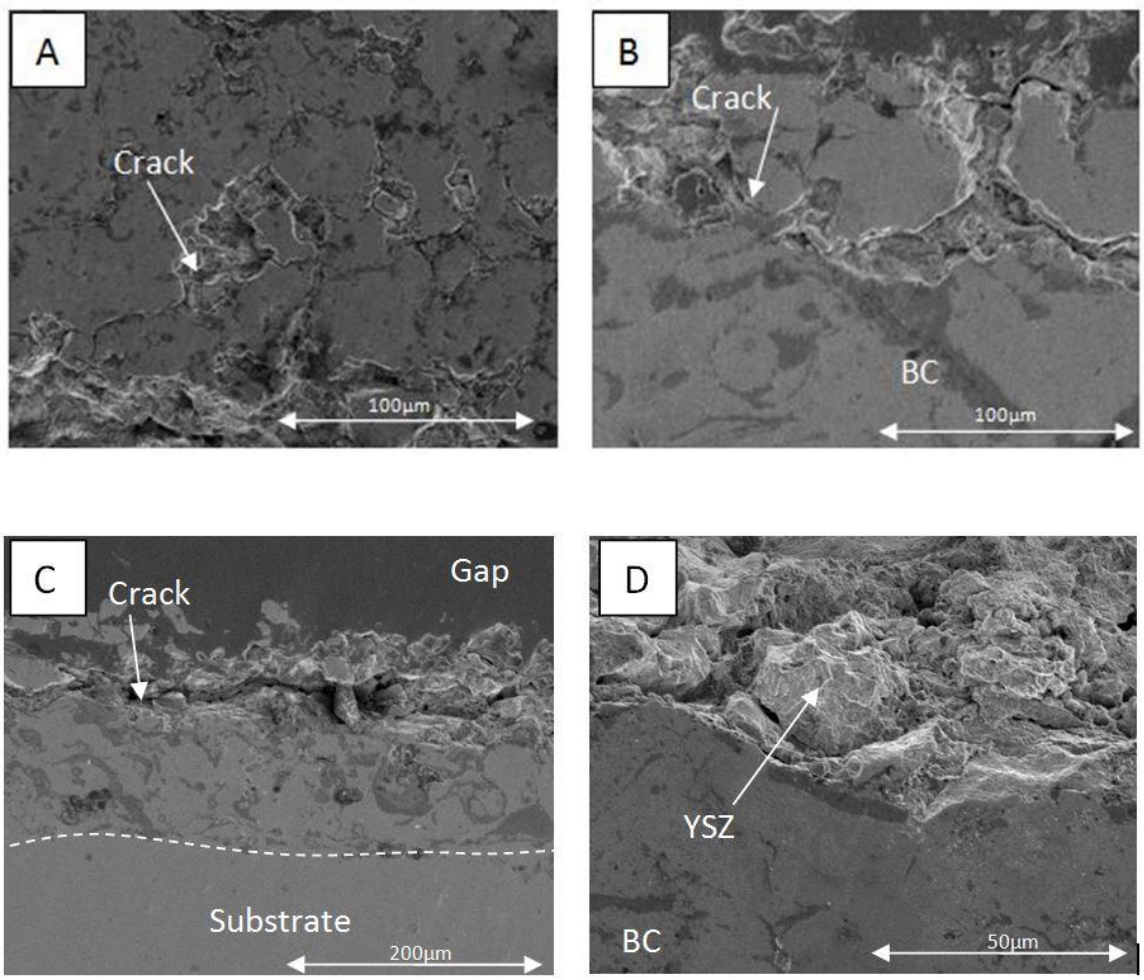

Figure 4.7 Micrographs of the cross section of the coatings after Isothermal thermal cycling tests on CM furnace (a) YSZ, (b) GZ, (c) 10%GZ/YSZ, (d) 25%GZ/YSZ

From figure 4.7, failure is observed in the bond coat/top coat interface in all the tested specimens. It is noted that the weakest location in typical YSZ TBCs is the interface of the bond coat/ top coat. Moreover, at high temperature, the chemical reaction between the top coat and the as formed thermally grown oxide (TGO) layer will dramatically reduce the performance of these TBCs. In Pure GZ coatings large cracks within the TBC close to the bond coat/ top coat interface are formed even without significant growth of thermally grown oxide (TGO). The low toughness of pure GZ ceramics seems to allow a crack growth even with lower stress levels. The premature failure of the pure GZ coatings can be mainly related to the chemical incompatibility of GZ coatings. It is also reasonable to suppose that low coefficient of thermal expansion (CTE) of GZ contributes to the increase of the residual stresses for cracking at the interface between bond coat and top coat when cooled down from operation temperature to ambient temperature. During cooling stress relaxation occurs as a function of coating thickness. Cracks in Double layer graded ceramic TBCs initiate because of the tensile stresses which are generated by cooling that follows relaxation of compressive stresses at high temperature.

Double layer TBCs failed at the bond coat/ top coat interface indicating that the failure is probably oxidation driven and not by limited temperature capability. The interfacial thermal stresses are the main factor for crack initiation and extension. If the

stress state exceeds the adhesive or cohesive bond strength of the coating, delamination and spallation may occur.

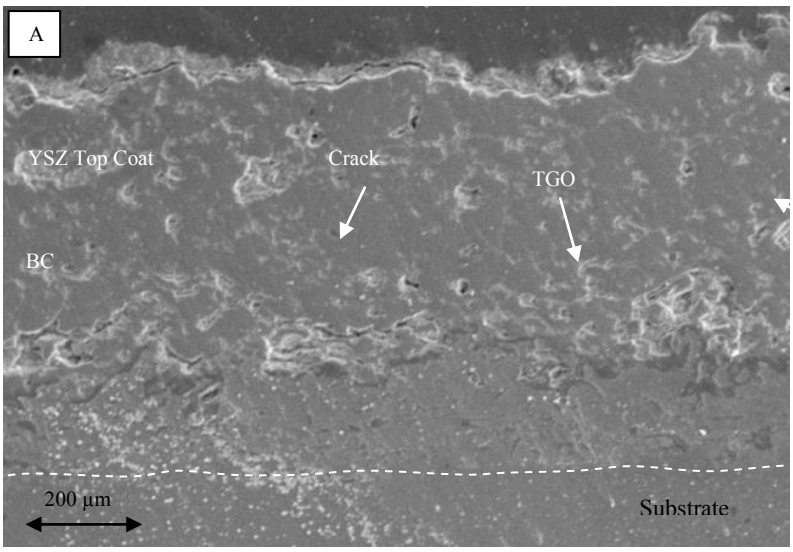

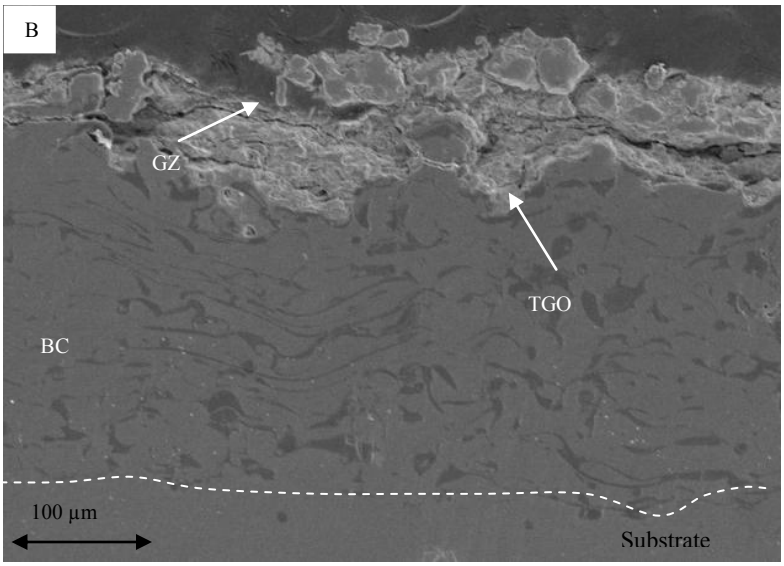

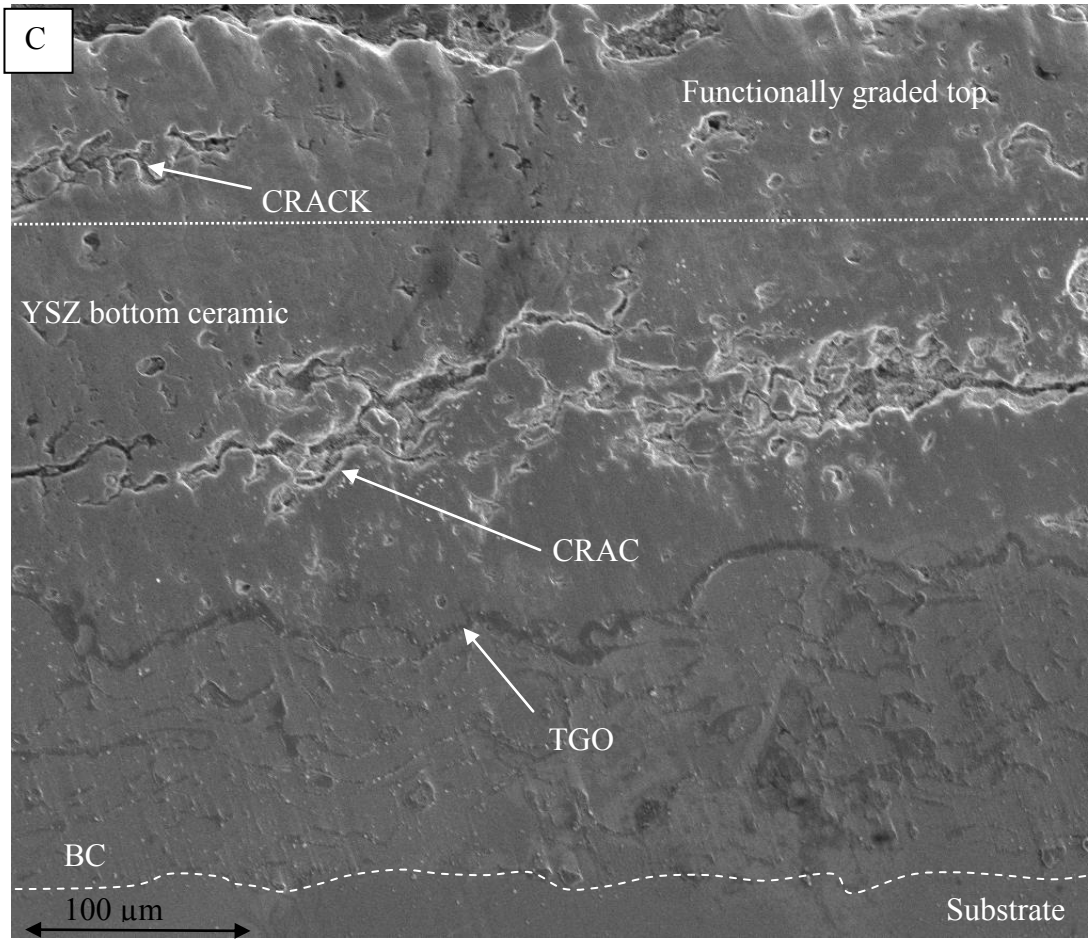

Figure 4.8 Micrographs of the cross section of the coatings after thermal gradient thermal cycling tests (a) YSZ, (b) GZ, (c) 50%GZ/YSZ

After thermal cycling a black thin layer with a thickness of ~10 µm between ceramic top coat and bond coat is clearly observed and this thin layer is called as the thermally grown oxide (TGO), implying that bond coat oxidation is important factor for coating failure. It is likely to deduce that thermal stresses in GZ are larger than that of YSZ due to the higher coefficient of thermal expansion of GZ than that of YSZ. More over considering the sintering effect of GZ and the reaction of GZ with TGO, thermal

cycling life of single layer GZ coatings is much shorter than that of single layer YSZ coatings. Growth stresses can be seen in the SEM images due to the oxidation of bond coat at high temperatures. Interfacial thermal stresses such as residual compression stresses lead to crack initiation and extension due to thermal shock, especially in the process of cooling down to the ambient temperature.

In the above coatings the cracks are initiated at the interface of the TGO layer and the top coat (Figure 4.8), which is a typical failure mechanism of TBCs. This means under the present cyclic conditions TBC failure is dominated by TGO thickening and cracking rather than by delamination cracking of ceramic top coat which is another failure mechanism.

Chapter V

SUMMARY AND CONCLUSIONS

In this thesis work the role of $Gd_2Zr_2O_7$ (GZ) powders in improving the life of thermal barrier coatings (TBCs) has been investigated. In addition to the examination of a unique new formulation of functionally graded GZ based double layer TBC systems a novel experimental testing process is presented to determine the relative merit of TBC coatings under thermal gradient cycling conditions. The functionality of this test method is described in detail and the general feasibility and applicability is confirmed.

Thermal cycling life and mechanical properties of functionally graded GZ+YSZ double layer TBCs in addition to pure YSZ and GZ TBCs are investigated and analyzed. All the samples used in this work are fabricated using standard air plasma spraying (APS) technique. The porosity of these TBCs is characterized quantitatively by mercury intrusion porosimetry using Poremaster 33 analyzer. Mechanical properties such as elastic modulus and hardness are measured by nano indentation on the cross-section of the coating specimens. The hardness test results indicated a trend of possible benefits of GZ addition up to 50% in the measured double layer TBCs. As the hardness and Young's modulus of 50% GZ/YSZ DL layered system is similar to that of YSZ it is reasonable to assume that GZ based functionally graded TBC system are expected to show superior thermal cycling life when compared to pure GZ TBCs while maintaining lower thermal conductivity than YSZ systems.

On the 1.45-hour Isothermal cycling, upon exposure to 1100^{o}C, life time of pure GZ coatings is well below compared to those of standard YSZ coatings. Functionally graded double layer systems showed significantly higher life time when compared to pure GZ coatings. Low coefficient of thermal expansion (CTE) of GZ contributes to the increase of the residual stresses for cracking at the interface between bond coat and top coat when cooled down from operation temperature to ambient temperature. In the double layer TBCs the failure occurred at the bond coat/ top coat interface indicating that the failure is probably oxidation driven and not by limited temperature capability.

On the 40 minutes temperature gradient thermal cycling, upon exposure to 1100^{o}C, pure GZ samples failed at ~200 cycles followed by functionally graded 50%GZ/YSZ double layer TBCs and pure YSZ TBCs at ~ 1500 cycles. The pattern is similar to the isothermal cycling tests but with improved cycles to failure due to the incorporation of temperature gradient in the thermal cycling process. One important advantages of this testing process is the failure of the TBC will not be dominated by the oxidation of the bond coat which provides room for more detailed examining capabilities about the other critical failure mechanisms such as crack initiation mechanisms, thermal fatigue behavior that may contribute to the failure of TBCs. The results of the temperature gradient thermal cycling indicate that at high surface temperatures (1100^{o}C) the functionally graded double layer 50%GZ/ YSZ TBC system meets the expectations, as the thermal cycling performance is similar to those of YSZ TBCs indicating that

addition of GZ in double layer TBC system improves the life of GZ based TBCs besides lower thermal conductivity thereby providing beneficial insulating TBC properties for high temperature applications.

Further investigation on the functionally graded GZ+YSZ double layer and multilayer TBC systems to improve the life of GZ based TBCs should be carried out in order for these materials to become visible in hot engine environment. Also, in future studies on the TBCs conditions not limited to high temperature, temperature gradient, high pressure, mass flow and thermal loading should be accommodated in the testing process to create a more realistic loading situation, closer to actual engine conditions.

BIBLIOGRAPHY

BIBLIOGRAPHY

1. Nitin P.Padture, Maurice Gell, Eric H.Jordan, Thermal Barrier Coatings for Gas-Turbine Engine Applications , *Science*., Vol 296, 2002, p 280-84.

2. Robert Vassen, Alexandra Stuke, and Detlev Stover, Recent Developments in the Field of Thermal Barrier Coatings, *Journal of Thermal Spray Technology.,* Vol 18(2), 2009, p 181-186.

3. Carlos G.Levi, Emerging materials and processes for thermal barrier systems, *Current Options in Solid State and materials Science.,* Vol 8, 2004, p 77-91.

4. Jie Wu,Xuezheg Wei, Nitin P.Padture, Paul G.Klemens, Maurie Gell, Eugenio Garcia, Pilar Miranzo and Maria I. Osendi, Low-Thermal-Conductivity Rare-Earth Zirconates for Potential Thermal-Barrier-Coating Applications, *Journal of the American Ceramic Society.,* Vol 85[12], 2002, p 3031-3035.

5. Xueqiang CAO, Application of Rare Earth in Thermal Barrier Coating Materials, *J.Mater Sci.Technol.*, Vol 23[1], 2007, p 15-35.

6. R.A.Miller, Thermal Barrier Coatings For Aircraft Engines: History and Directions, *Journal for Thermal Spray Technology.,* Vol 6 [1], 1997, p35-42.

7. R.Vaben, E Traceger, D.Stover, New Thermal Barrier Coatings Based on Pyrochlore/YSZ Double-Layer Systems, *International Journal of Applied Ceramic Technology*, Vol 1[4], 2004, p 351-361.

8. Prakash C.Patnaik, Xiao Huang, Jogender Singh, State of the Art and Future Trends in the Development of Thermal Barrier Coating Systems, *Innovative Missile Systems.*, Vol 38, 2006, p 1-20.

9. D. Stöver, G. Pracht, H. Lehmann, M. Dietrich, J-E. Döring, and R. Vaßen, New Material Concepts for the Next Generation of Plasma-Sprayed Thermal Barrier Coatings, *Journal for Thermal Spray Technology.,* Vol 13 [1], 2004, p76-83.

10. Kee Sung Lee, Kyu Luk Jung, Yong Suk Heo, Tae Woo Kim, Yeon-Gil Jung, Ungyu Paik, Thermal and mechanical properties of sintered bodies and EB-PVD layers of Y_2O_3 added $Gd_2Zr_2O_7$ ceramics for thermal barrier coatings, *Journal of Alloys compounds.,* Vol 507, 2010, p 418-455.

11. Mohamed N. Rahaman, Jacob R. Gross, Rollie E. Dutton, Hsin Wang, Phase stability, sintering, and thermal conductivity of plasma-sprayed ZrO2–Gd2O3 compositions for potential thermal barrier coating applications, *Acta Materialia.,* Vol 54, 2006, P 1615-1621.

12. Andrew D.Gledhill, Kongara M.Reddy, Julie M.Drexler, Kentaro Shinoda, Sanjay Sampath, Nitin P.Padture, Mitigation of damage from molten fly ash to air-plasma-sprayed thermal barrier coatings, *Materials science and Enginnering.*, Vol A 528, 2011, p 7214-7221.

13. Tanja Stinke, Doris Sebold, Daniel E.Mack, Robert Vaben, Detlev Stover, A novel test approach for plasma-sprayed coatings tested simultaneously under CMAS and thermal gradient cycling conditions, *Surface & Coating Technology*., Vol 205, 2010, p 2287-2295.

14. Zhenhua Xu, Shimei He, Limin He, Rende Mu, Guanghong Huang, Xueqiang Cao, Novel thermal barrier coating based $La_2(Zr_{0.7}Ce_{0.3})_2O_7$/8YSZ double-ceramic-layer systems deposited by electron beam physical vapor deposition, *Journal of Alloys and Compounds.,* Vol 509, 2011, p 4273-4283.

15. David R.Clarke, Material selection guidelines for low thermal conductivity thermal barrier coatings, Surface *and Coatings Technology.,* Vol 163-164, 2003. p 67-74.

16. P.G. Klemens, M. Gell, Thermal conductivity of thermal barrier coatings, Materials Science and Engineering., Vol A245, 1998, p-143-149.

17. Robert Vassen, Holger Kassner, Alexandra Stuke, Daniel Emil Mack, Maria Ophelia Jarligo and Detlev Stover, Functionally Graded Thermal Barrier Coating with Improved Reflectivity and High-Temperature Capability, *Materials Science Forum.,* Vol 631-632, 2010, p 73-78.

18. Dae-Jin Kim, sung-Keun Cho, Jung-Hun Choi, Jae-Mean Koo, Chang-Sung Seok and Moon-Young Kim, Evaluation of the degradation of Plasma Sprayed Thermal barrier Coatings Using Nano-Indentation, *Journal of Nano Science and nanotechnology.,* Vol 9 [12], 2009, p 7271-7277.

19. N.Zotov, M.Barsch, G.Eggeler, Tehrmal barrier coating systems- analysis of nanoindentation curves*, Surface & Coatings Technology.,* Vol 203, 2009, p 2064-2072.

20. Hongbo guo, Hongju Zhang, guohui Ma, Shengakai Gong, Thermo-physical and cycling properties of plasma-sprayed $BaLa_2Ti_3O_{10}$ coating as potential thermal barrier, *Surface and Coatings Technology*., Vol 204, 2009, p 691-696.

21. K.A.Khor, Y.W.Gu, Thermal properties of plasma-sprayed functionally graded thermal barrier coatings,*Thin solid Films.,* Vol 372, 2000, p 104-113.

22. A.Portinha, V.Teixerira, J.Carneiro, J.Martins, M.F.Costa, R.Vassen, D.Stoever, Characterization of thermal barrier coatings with a gradient in porosity, Surface& Coatings Technology 195(2005)245-251.

23. Ann Bolcavage, Albert Feuerstein, Jhon Foster and Peter Moore, Thermal Shock testing of Thermal Barrier Coating/Bondcoat Systems, *Journal of Materials Engineering and Performance.,* Vol 13 [4], 2004, p 389-397.

24. K.Kokini, Y.R.Takeuchi&B.D.Choules, Thermal Crack Initiation mechanisms on the Surface of Functionally Graded Ceramic Thermal Barrier Coatings , *Ceramics Internationa.,l* Vol 22, 1996, p 397-401.

25. Y. Liu, C. Persson, and S. Melin, Fracture Mechanics Analysis of Microcracks in Thermally Cycled Thermal Barrier Coatings, *Journal for Thermal Spray Technology.,* Vol 13 [3], 2004, p377-380.

26. Progress in Thermal Barrier Coatings, The American Ceramic Society, A John Wiley & Sons, Inc., Publication, 2009.

27. O.A.Agu, Charecterization and Analysis of Advanced Microstructured Thermal Barrier Coating (TBC) for Elevated Temperature Applications, *Master's Thesis.*, Department of Mechanical Engineering, Southern University and A&M College, July 2010.

28. M.B.Sliva, Study of microstructure effect on the thermal properties of yattria-stabilized-zorconia thermal barrier coatings made by atmospheric plasma spray and pressing machine, *PhD Dissertation.*, Department of Mechanical Engineering, Louisiana State University, May 2010.

29. N.Polasa, A study of temperature oxidation and hot corrosion of advanced multilayer thermal narrier coatings, *Master's Thesis.*, Department of Mechanical Engineering, Southern University and A&M College, December, 2010.

30. L. Wang, S. Nandikolla, M. H. Habibi, P. F. Mensah, R. Diwan, and S. M. Guo, Thermal Cycling Behavior of $Gd_2Zr_2O_7$ Based Thermal Barrier Coatings, *Materials Science & Technology Conference and Exhibition*, 2011, p-1046-1053.

VITA

Mr. Swamy Nandikolla was born in Kakinada, India in 1987. He received a Bachelor's Degree in Mechanical Engineering from Jawaharlal Nehru Technological University, Hyderabad, India in 2008. He later worked at G M R Power Corporation Private Limited, Vemagiri, India as an operations supervisor between 2008 and 2009 before arriving in United States to peruse his Master's Degree. Mr. Swamy joined Southern University and A&M college as a graduate student in August 2010. While on the graduate program in Mechanical Engineering (Thermal Science), Mr. Swamy worked as a graduate assistant in on-going research activities for Dr.Mensah in the area of developing a novel testing method for testing Thermal Barrier Coatings for high temperature applications.

_____

Signature

APPROVAL OF SCHOLARLY DISSEMINATION

The author grants to the Southern University Library the right to reproduce, by appropriate methods, upon request, any or all portions of this thesis.

It is understood that "request" consists of the agreement, on the part of the requesting part, that said reproduction is for his personal use and the subsequent reproduction will not occur without written approval of the author of this thesis.

The author of this thesis reserves the right to publish freely, in the literature, at any time, any or all portions if this thesis.

Author _____

Date _____